Chapter 1

Introduction

1.1 Overview of Low temperature poly-silicon thin-film transistors (LTPS TFTs)

As the popularization of flat panel displays grows up, liquid-crystal displays (LCDs) have become the most common system in many commercial applications. Low temperature poly-silicon (LTPS) thin-film transistors (TFTs) is one of the extremely important electronic devices because of their numerous applications in liquid-crystal displays (LCDs)

More recently, high-end flat panel display is what we are pursuing. Sensor on panel is one of value-added functions for display panel. Various sensors are created on panel such as ambient light sensor, image sensor, gas sensor and so on [1-2]. Some of sensors were integrated to peripheral area of glass substrate of panel and some integration to pixel. [3]

1.2 Motivation

Temperature is an important factor in a display system [4]. One of the obvious influences is the effective dielectric anisotropy (△ε) of liquid crystal capacitance. As shown in Fig. 1-1. In this figure, the molecules wiggle less and △ε is large at cold temperatures. At warmer temperatures, △ε is reduced. Then at and above the clearing temperature, order breaks down and the material becomes isotropic (△ε=0). And capacitor changes, together with the dielectric constant. Change in the liquid crystal capacitor changes will affect the rotational angle of the molecules and its

transformation. When we are driving pixel, the changes of transformation will let us get the wrong colors. Since we are using the same data voltage for driving. At warmer temperatures, we must rectify the gamma curves to get the right colors. A temperature sensor is needed.

About temperature sensors, we have thermal couple, thermally sensitive resistance, thermal IC and so on. No matter what kind of sensor we used, we all need additional cost.

In this thesis, we propose a temperature sensor directly using LTPS TFTs identically fabricated with the pixel TFT. So we don't need any additional cost. Besides, LTPS TFTs with poor uniformity, even consider fabricated under the identical process, we also propose a calibration method which can reduce errors [5].

1.3 Thesis Organization

Chapter 1 Introduction

1.1 Overview of Low temperature poly-silicon thin-film transistors (LTPS TFTs)

1.2 Motivation

1.3 Thesis Organization

Chapter 2 Thermal Effect of Device

2.1 Procedures of Fabricating LTPS TFTs

2.2 Device Characteristic

2.3 Device Variation

2.4 Summary

Chapter 3 Temperature Sensor Circuit

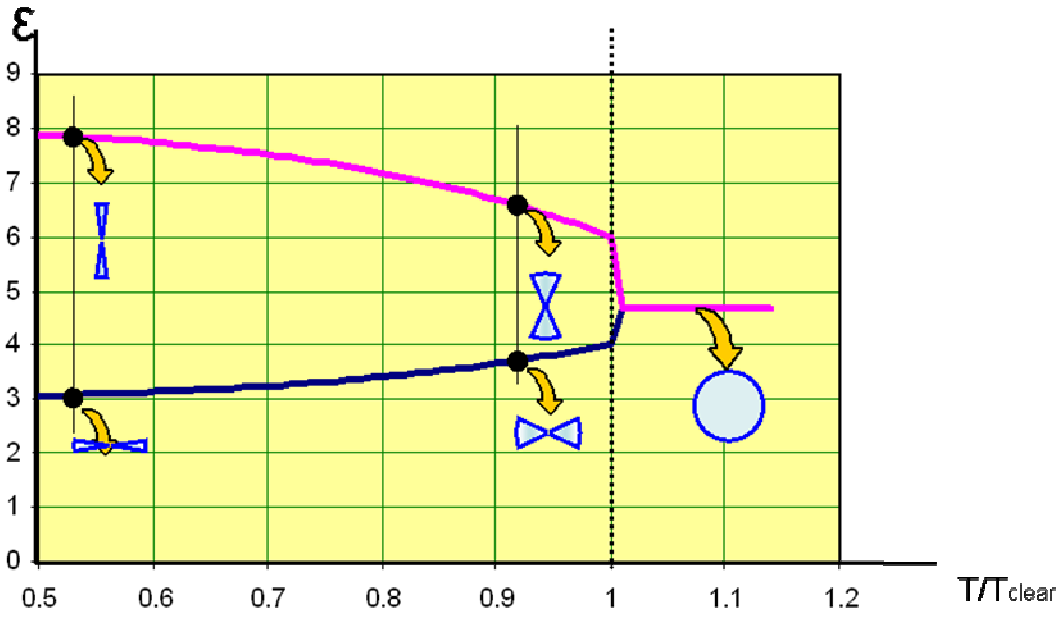

Fig. 1-1. The effective dielectric of liquid crystal changed from anisotropic to isotropic behavior with temperature.

Chapter 2

Thermal Effect of Device

2.1 Procedures of Fabricating LTPS TFTs

The LTPS TFTs used in this thesis were the conventional top-gate n-type poly-Si TFTs with lightly doped drain (LDD) and fabricated on the glass substrates. Fig. 2-1 shows the cross-section views of LTPS TFTs. Firstly, the buffer oxide and a-Si:H film was deposited on glass substrates with PECVD. The samples were then put in the oven for dehydrogenation. The XeCl excimer laser was applied. The laser scanned the a-Si:H film to recrystallize the a-Si:H film to poly-Si. After poly-Si active area definition, 65 nm SiO_2 was deposited with PECVD as the gate insulator. Next, the metal gate was formed by sputter and then defined. The LDD and the n_+ source/drain doping were formed. Then, the interlayer of SiN_x was deposited. Subsequently, the rapid thermal annealing was conducted to activate the dopants. Meanwhile, the poly-Si film was hydrogenated. Finally, contact hole formation and metallization were performed to complete the fabrication work. In this study, the TFTs having a channel width (W) of 20 μm and a channel length (L) of 5 μm with a LDD structure of length 2 μm are measured in chapter 2. And in chapter 3, different dimension (W/L=400μm /8μm) will be used.

2.2 Device Characteristic

Fig. 2-2 shows that the device characteristics in different temperatures. The device characteristics include saturation region and linear region. In order to investigate in detail the characteristics, It will be divided into three regions were on

region, sub-threshold region and off region.

In on region, the drain current increase at warmer temperatures as show in Fig. 2-3. In this figure we select the drain current at V_G =7V. At 25℃, the drain current is 0.342 mA in high V_{DS} region (V_{DS}=10V) and 3.42 μA in low V_{DS} region (V_{DS}=0.1V). At 80℃, the drain current is 0.357mA in saturation region and 7.97μA in linear region. In this region, the drain current ratio is 1.04 and 2.33.

In sub-threshold region, thermal effect is obvious than on region. Fig. 2-4 shows the drain current change from 25℃ to 80℃. No matter in high V_{DS} or low V_{DS} the maximum of the drain current ratio is over 26. In off region, low V_{DS} will be excluded. Because of the drain current is small as close to noise as show in Fig. 2-5. Then we select the drain current at V_G = -2V. The drain current is from 1.61 pA to 27.3 pA. The ratio is 16.94.

Fig. 2-6 shows the drain current in 25℃ and the proportion of 80℃ at V_{DS} = 0.1V, 10V. So we can see that thermal effect is unobvious when device turn on. As for temperature sensor, sub-threshold region and off region are relatively feasible.

2.3 Device Variation

LTPS TFTs have attracted much attention for the higher mobility and better reliability compared to amorphous silicon thin-film transistors [6]. However, even the devices fabricated under the identical process, LTPS TFTs still have different electrical characteristics.

Fig. 2-7 shows the 200 current-voltage characteristic curves of LTPS TFTs at V_{DS}=10V. The differences can be divided into two, one is threshold voltage variation and the other one is off current variation. In Fig. 2-6 we can see that the current ratio changes very sensitive in sub-threshold region. Therefore, even if threshold voltage

changes little, the current ratio changes are still great. So when we consider threshold voltage variation, sub-threshold region as a temperature sensor is inappropriate. But in off region, the variation is acceptable. About the effect of off current variation, we will discuss in the section 3-2-1.

2.4 Summary

According to the experiment before, the most obvious effect of temperature is in sub-threshold region but threshold voltage shift is the inevitable problem. And in on region thermal effect is unobvious. So as for temperature sensor, off region current is chosen.[7]

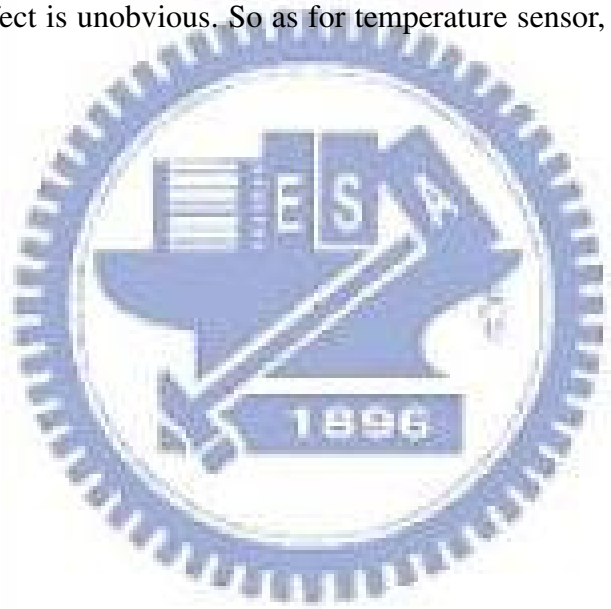

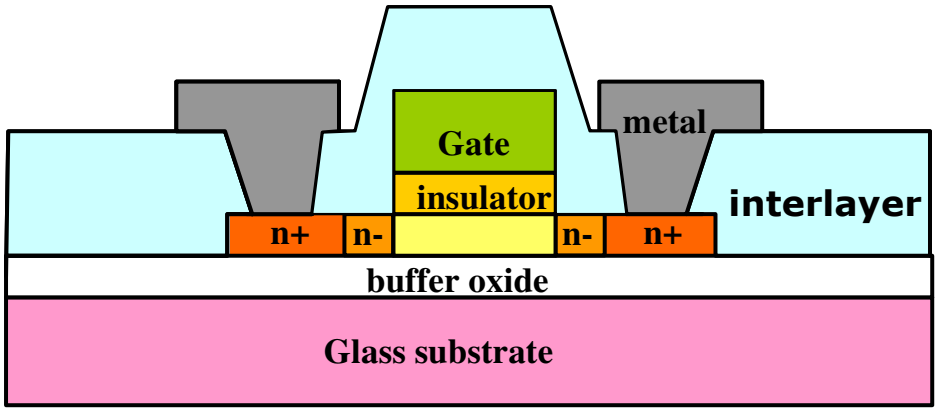

Fig. 2-1. Illustrates a cross-section view of a LTPS TFT.

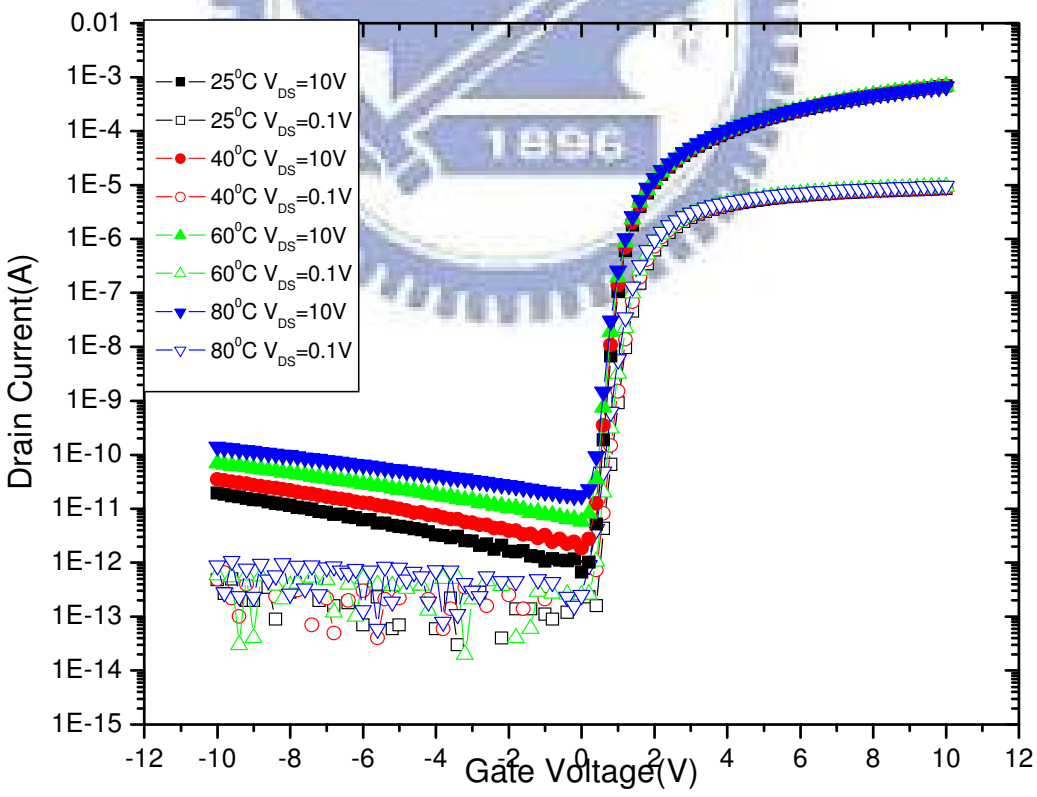

Fig. 2-2. Illustrates a current-voltage characteristic of a LTPS TFT at different temperatures.

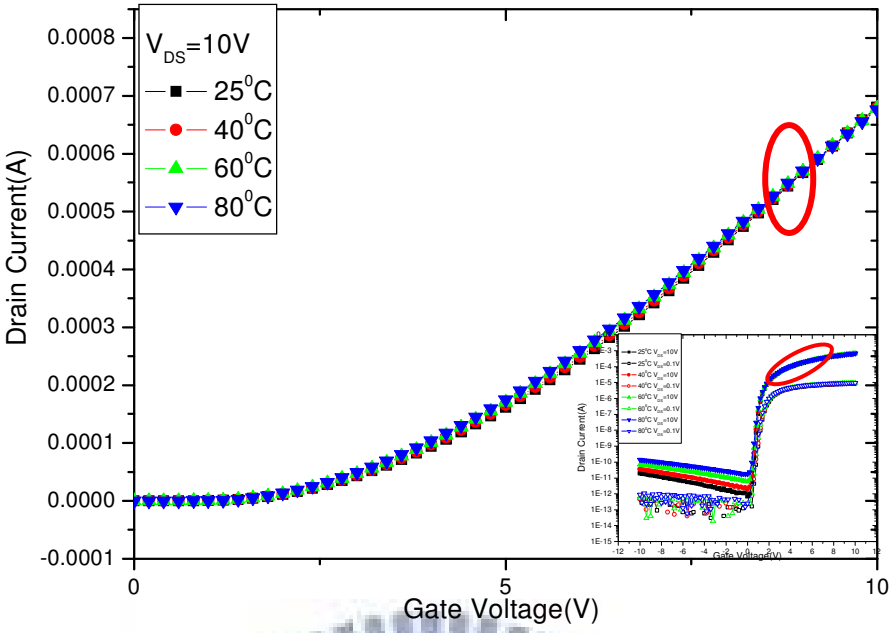

Fig. 2-3(a) In on region, temperature dependence of current-voltage characteristic at V_{DS} = 10V.

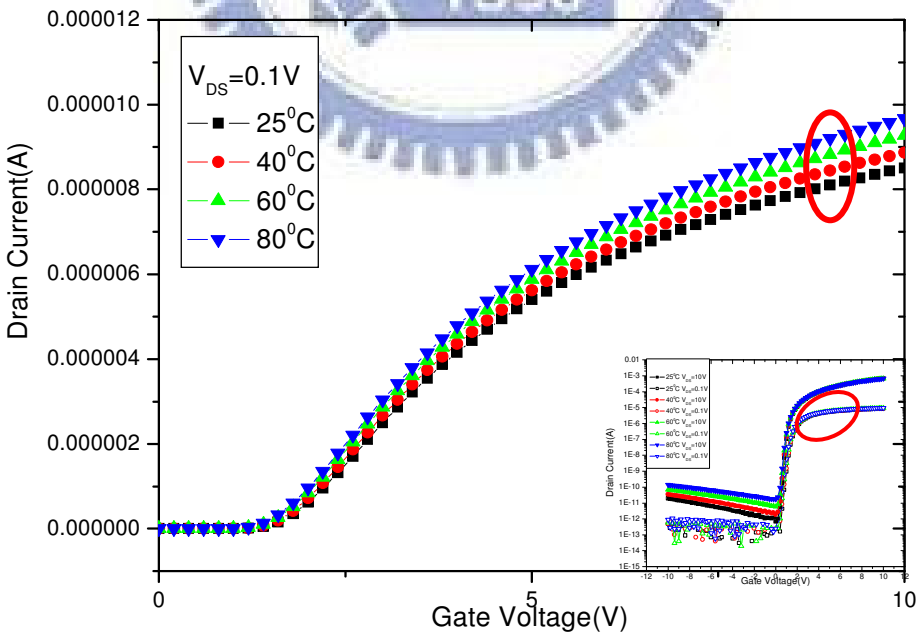

Fig. 2-3 (b) In on region, temperature dependence of current-voltage characteristic at V_{DS} = 0.1V

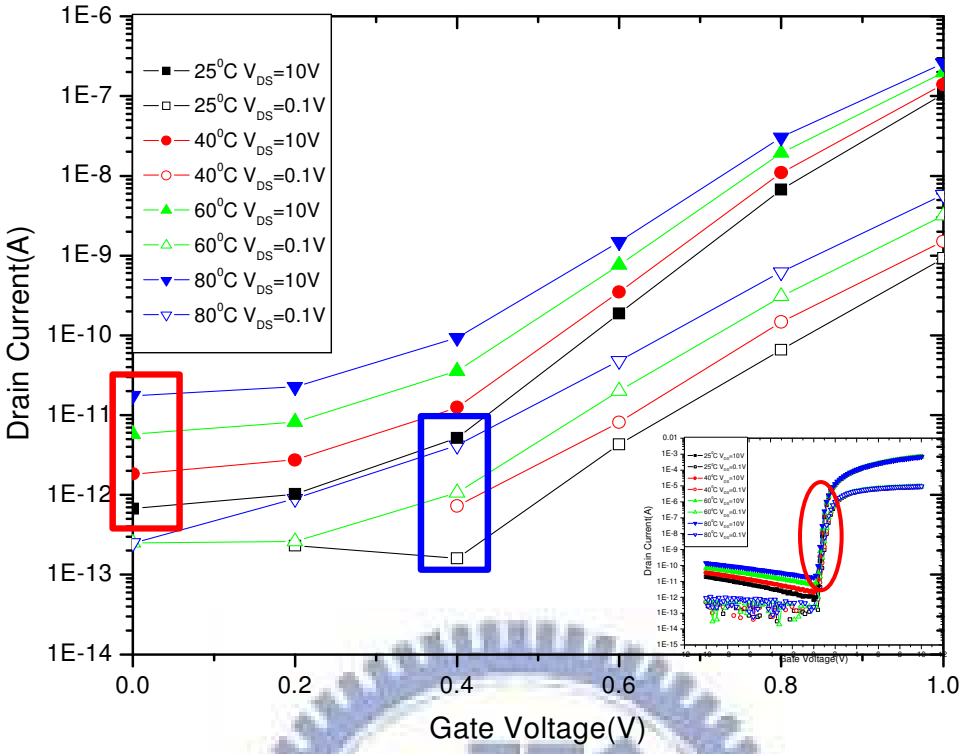

Fig. 2-4 In sub-threshold region, temperature dependence of current-voltage characteristic at V_{DS} = 0.1V, 10V.

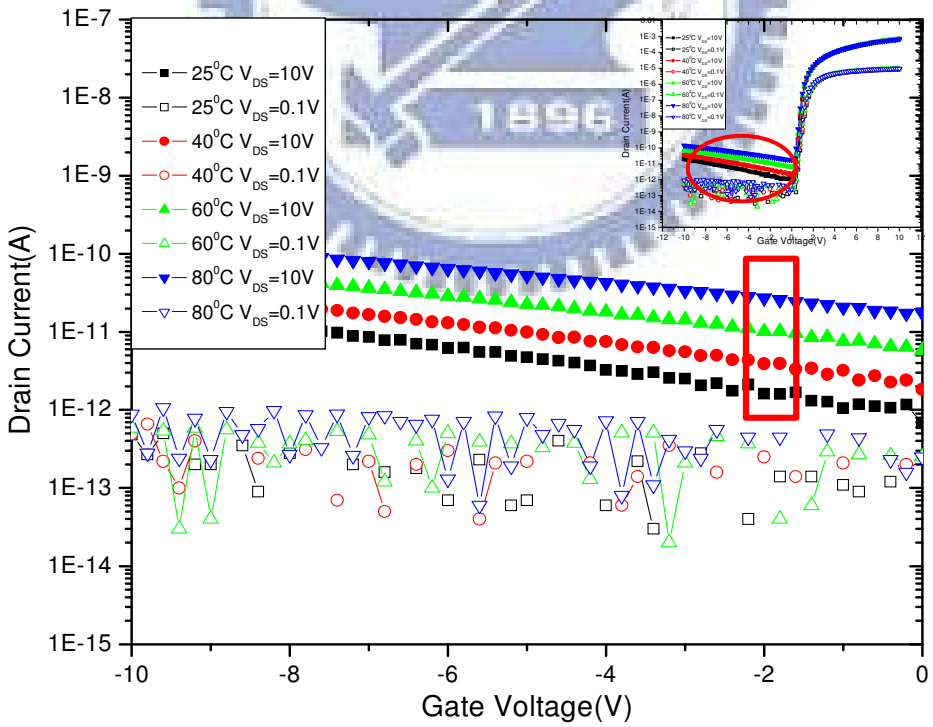

.

Fig. 2-5 In off region, temperature dependence of current-voltage characteristic at V_{DS} = 0.1V, 10V

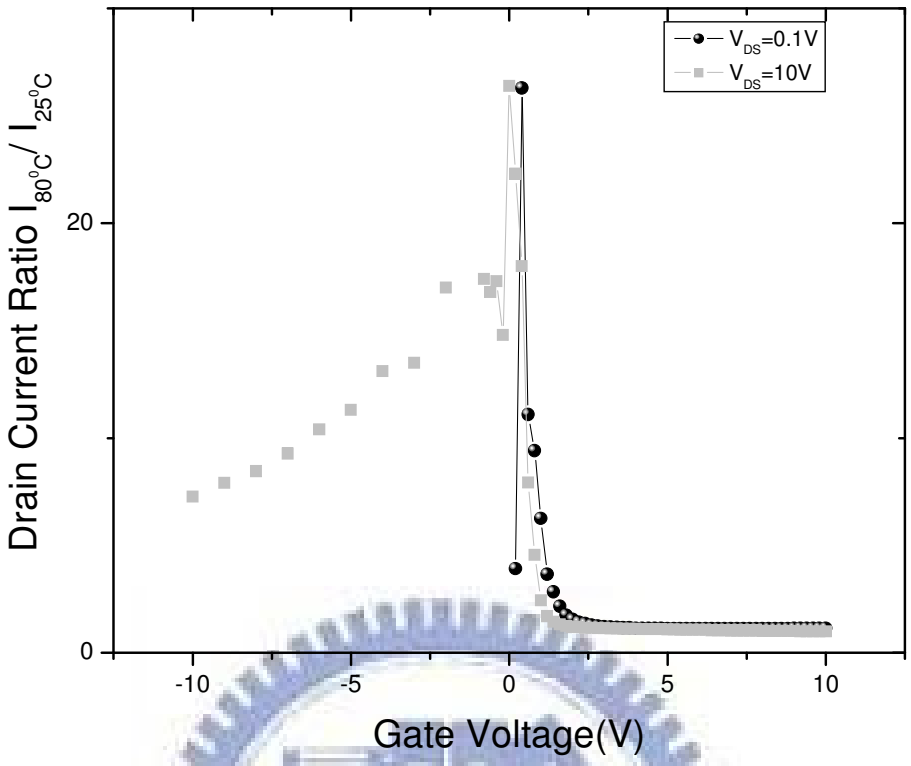

Fig. 2-6 The drain current in 25℃ and the proportion of 80℃ at V_{DS} = 0.1V, 10V.

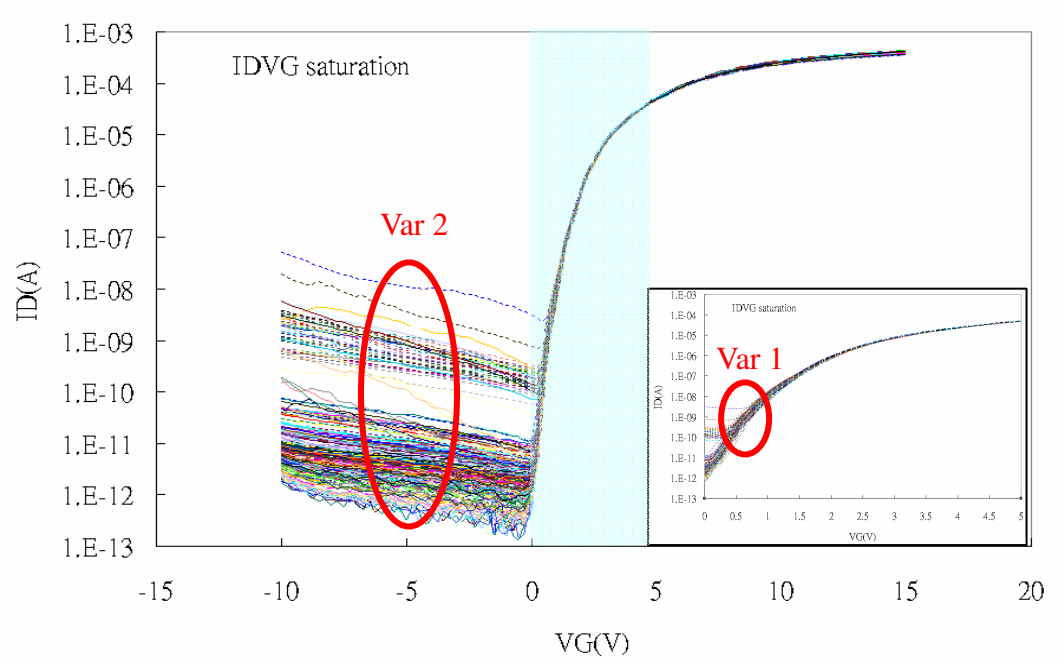

Fig. 2-7 The 200 current-voltage characteristic curves of LTPS TFTs at V_{DS}=10V. The box represent the local enlarge of sub-threshold region. (Var 1: threshold voltage variation, Var 2: off current variation)

Chapter 3

Temperature Sensor Circuit

After the discussion of the thermal effect in chapter 2, we decide to use off region current as the signal of temperature, and focus on its thermal characteristic. Therefore, we propose a temperature sensor which can sense the changes of off region current at different temperatures.

3.1 Principle of Circuit

To use the off region current, we propose a 1T1C temperature sensor and its timing diagram as shown in Fig. 3-1. The proposed circuit here is all constructed with LTPS TFTs. The T1 functions as a switch and also a temperature sensing element, where the Cs is a storage capacitance. The sensing sequence consists of charge period and discharge period as following.

In charge period, T1 functions as a switch. When Vg becomes “Vg high”, T1 turn on. At this time, node A is charged to Vdata as “Vdata high”. In discharge period, Vg becomes “Vg low” and Vdata turns into zero, when T1 turn off. In this period, T1 is in the off region and the current that go through T1 was leakage current. As discussed before, the off region current will increase when the temperature rises. And the voltage of node A (V_A), which is supported by Cs, will be discharged due to the leakage current of T1. In other words, V_A drops faster at warmer temperatures. Therefore, we can get temperatures from the speed of voltage drop.

In actual application, in order to know V_A, we must acquire the voltage at node A. But if we put a real probe on node A, charges may get lost because of the probe

load if the impedance of the probe is not large enough. In order to avoid this problem, an embedded OP can be a solution [11]. However OP fabricated on glass occupies too large area to be incorporated in pixel. Therefore we convert leakage current to analog voltage signal by adding the T2 TFT as a source follower as shown in Fig. 3-2 [8, 9].

3.2 Source Follower

Source follower is a FET amplifier in which signal is applied between gate and drain with output taken between source and drain. A conventional source follower is shown in Fig. 3-3(a). Ideally the relationship between V_{in} and V_{out} can be expressed

$$V_{out} = V_{in} - V_{th}. \quad (1)$$

Now we want to use the source follower to convert leakage current to analog voltage signal. Firstly, we should make sure that the electrical characteristic of source follower is dependable. We use a triangular wave as the input signal for test and the output signal indeed remains the waveform as shown in Fig. 3-3(b). We further observe the frequency response of the source follower. We input a triangular wave which is from 2V to 9V and observe the highest and the lowest output signal voltages as shown in Fig. 3-3(c). In this figure, we can see that the output signal waveforms distort in the frequency above 100Hz. So for the proper operating of the source follower, we use 100Hz in this thesis.

Next we consider the temperature dependence of the source follower. Fig. 3-4 shows the output voltages of the source follower at different temperatures. The difference is less than 0.2V when the temperature increases to 80℃ and the difference of slope is only 1.3%. The source follower works in on region and the thermal effect is unobvious in this region. Therefore the source follower won't affect the measuring results of the device leakage at different temperatures. In addition, the

output voltage slope is 0.9 time of the input voltage slope.

3.3 Experimental Results

The picture of the proposed sensor fabricated on glass using LTPS technology is shown in Fig. 3-5(a). The output voltage of proposed sensor is measured under temperature varying from 25 to 80℃. The waveforms at 25 and 80℃ are shown in Fig. 3-5(b) and Fig. 3-5(c) respectively. In these two figures, in discharge period, the change of V_{out} is obvious at different temperatures, the slope at 80℃ is steeper than 25℃. So we can determine the temperature from the slope of V_{out}. When the slopes of V_{out} multiplied by storage capacitance, the results are the leakage currents according to the equation

$$I_{leakage} = \frac{dV_{out}}{dt} Cs = 0.9 \frac{dV_A}{dt} Cs . \quad (2)$$

Before we explain Eq. (2), we discuss with the temperature dependence of I_D - V_D characteristics as shown in Fig. 3-6. In this figure, the drain current increase at warmer temperatures and it can be expressed as

$$I(T) = A(T)(V_D - V_0(T)), \quad (3)$$

where A(T) is temperature dependent. After that the results of Eq. (2) can be expressed by formula as follows:

$$C \cdot V = I \cdot t \quad (4)$$

From Eq. (4)

$$A(T) \cdot (V_A(t) - V_0(T)) = Cs \cdot \frac{dV_A(t)}{dt}$$

$$\Rightarrow V_A(t) = \alpha \cdot e^{\frac{A(T)}{Cs}t} + V_0(T) . \quad (5)$$

Express Eq. (5) by Taylor series:

$$V_A(t) = \alpha \cdot [1 + \frac{A(T)}{Cs}t + \frac{1}{2}(\frac{A(T)}{Cs}t)^2 + ...] + V_0(T) . \quad (6)$$

Because of our design,

$$\frac{A(T)}{Cs} << 1 \quad \text{and} \quad \alpha = V_A(0) - V_0(T),$$

Where $V_A(0)$ is the initial voltage of discharge period. Therefore, Eq. (6) can be simplified as

$$\begin{aligned} V_A(t) &= \alpha \cdot [1 + \frac{A(T)}{Cs} t] + V_0(T) \\ &= V_A(0) - V_0(T) + \frac{A(T)}{Cs} \cdot V_A(0) \cdot t - \frac{A(T)}{Cs} \cdot V_0(T) + V_0(T) \\ &= V_A(0) + \frac{I(T)}{Cs} t \end{aligned} \tag{7}$$

From Eq. (1) we know that

$$V_{out}(t) = V_A(t) - V_{th} \tag{8}$$

Therefore, the slope of V_{out} multiplied by storage capacitance is the leakage current. After calculating the slopes at different temperatures, we can get the temperature dependence leakage currents as shown in Fig. 3-7.

3.4 Digitization

In order to avoid noise, we need convert the slope of V_{out} to digital signal. Fig. 3-8(a) is a digitization circuit we proposed. We use two comparators, one logic gate and one counter in this circuit. V1 and V2 are two reference voltages which are used to judge the range of V_{out}. Because of the logic gate C, the counter will get signals from CLK when V1> V_{out} >V2 as shown in Fig. 3-8(b), and the counter number can reflects the slope of V_{out}.

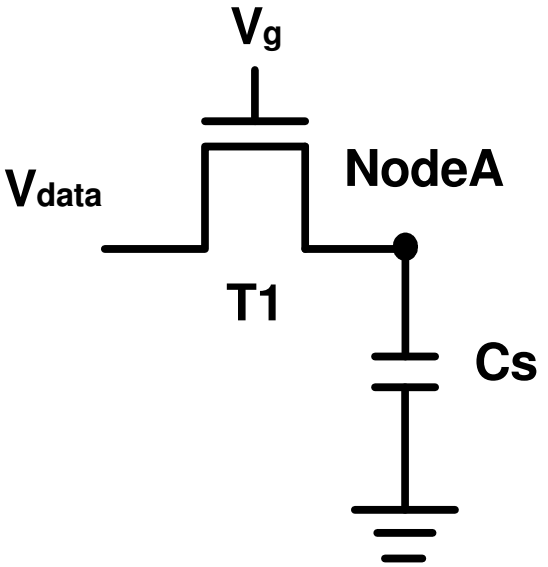

(a)

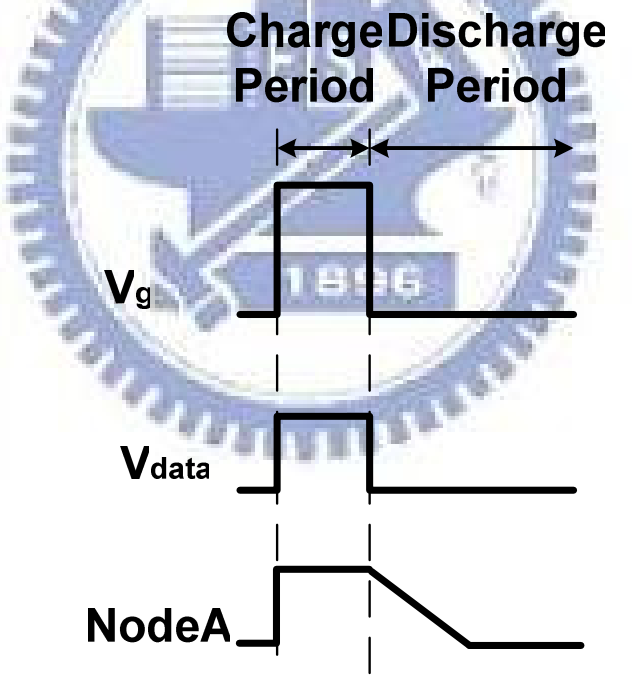

(b)

Fig. 3-1 (a) Schematic diagram of proposed 1T1C temperature sensor and (b) timing diagram.

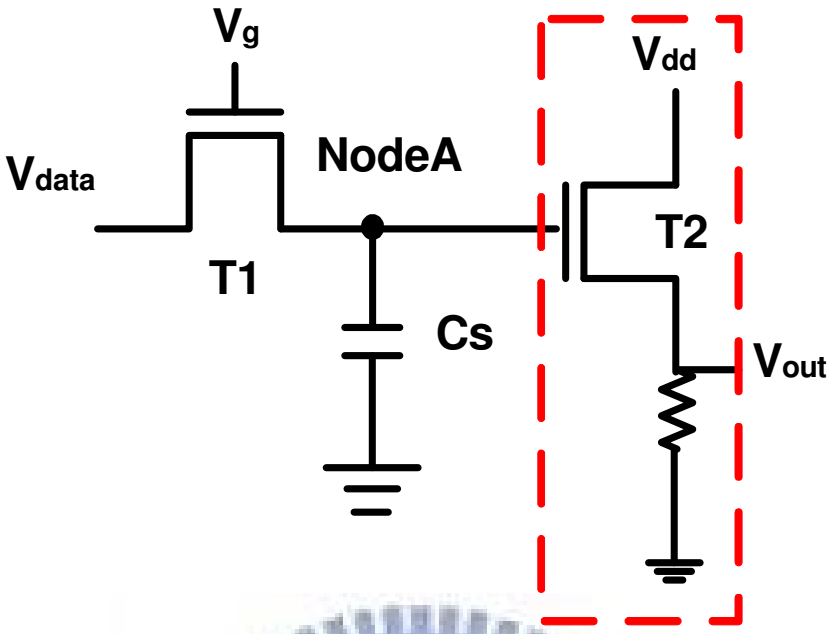

(a)

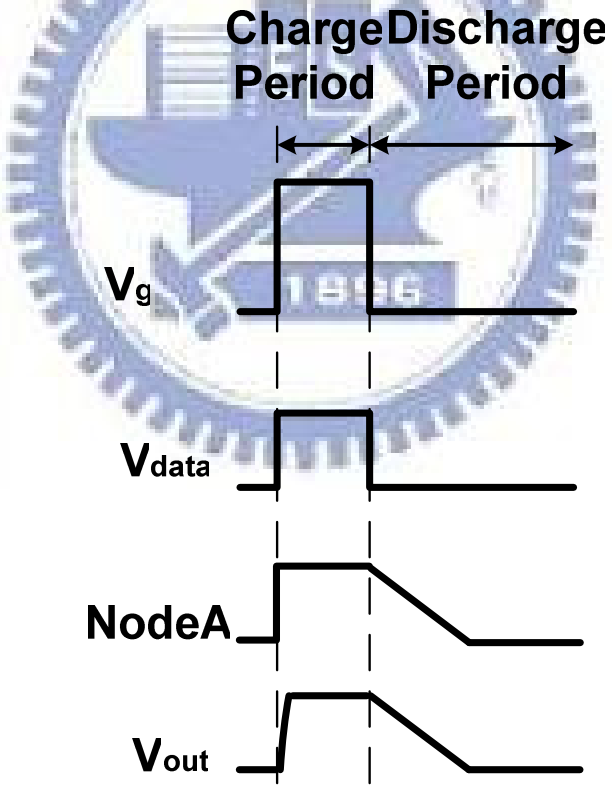

(b)

Fig. 3-2 (a) Schematic diagram of proposed 2T1C temperature sensor and (b) timing diagram.

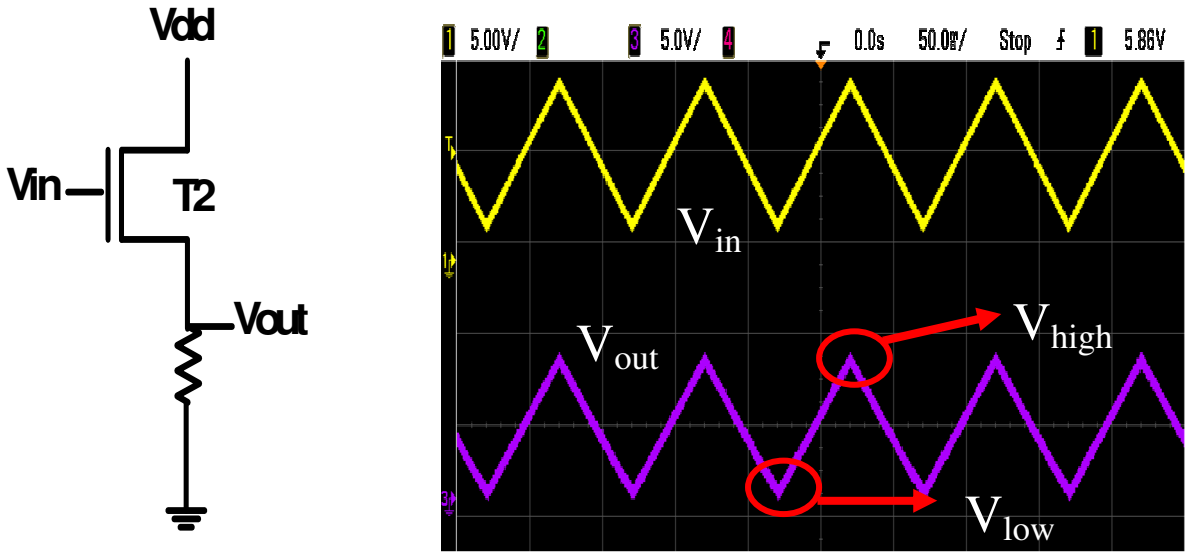

(a) (b)

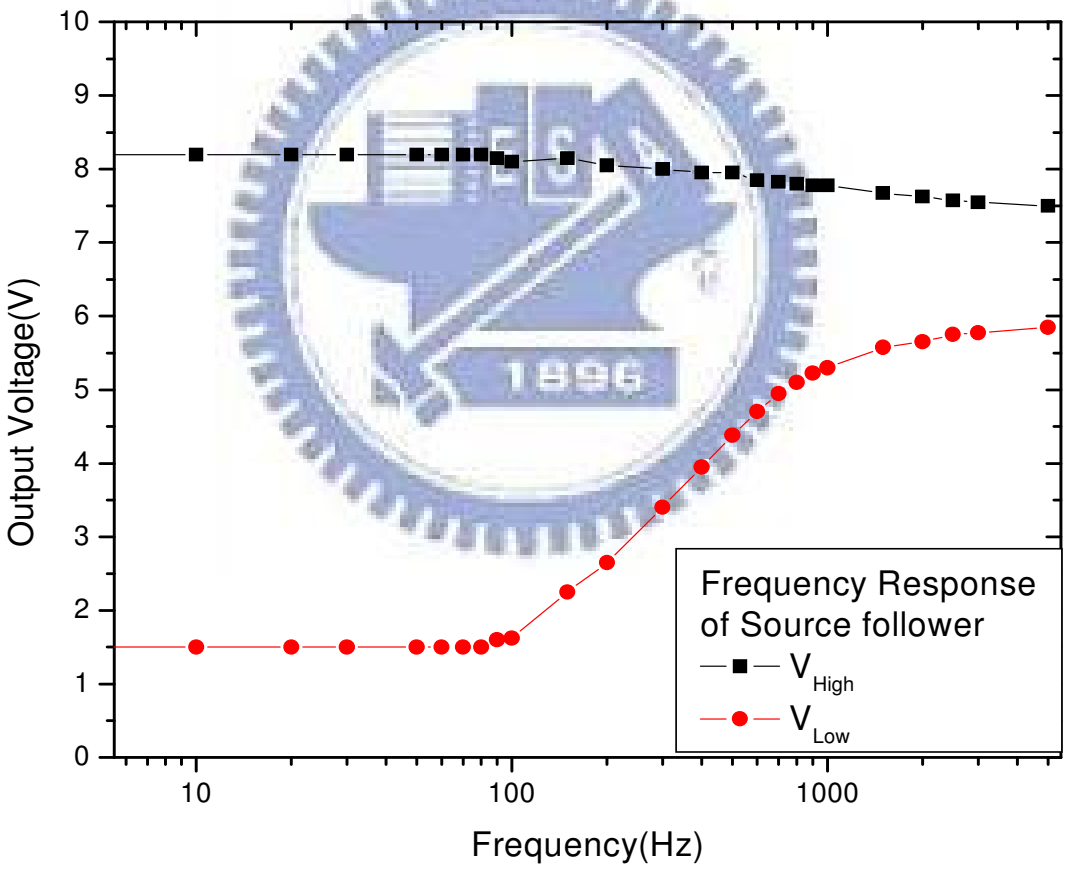

(c)

Fig. .3-3 (a) The conventional source follower. (b) The input and output signal waveforms of source follower. (c) The relationship between output waveform and input frequencies, when the input triangular wave is from 2V to 9V.

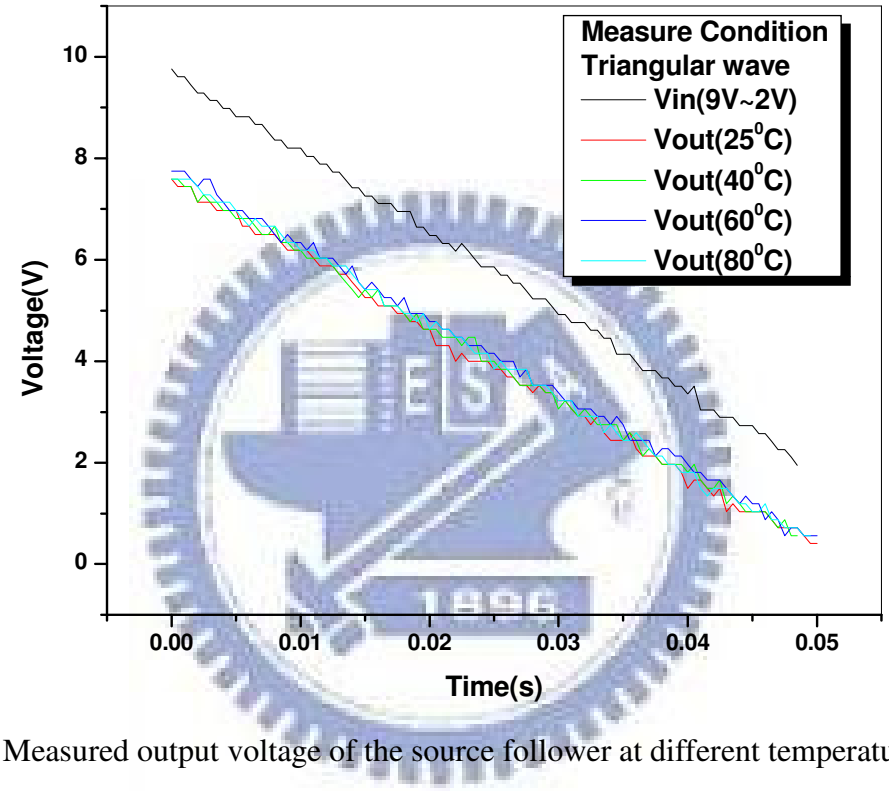

Fig. 3-4 Measured output voltage of the source follower at different temperatures.

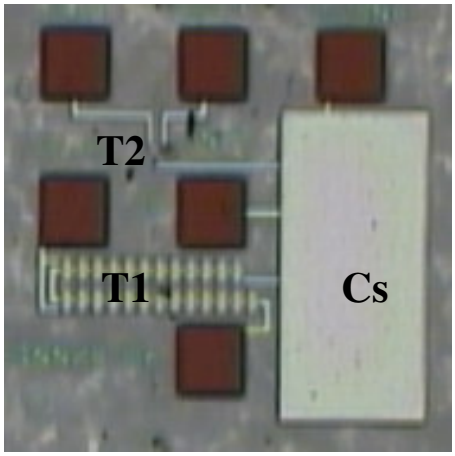

(a)

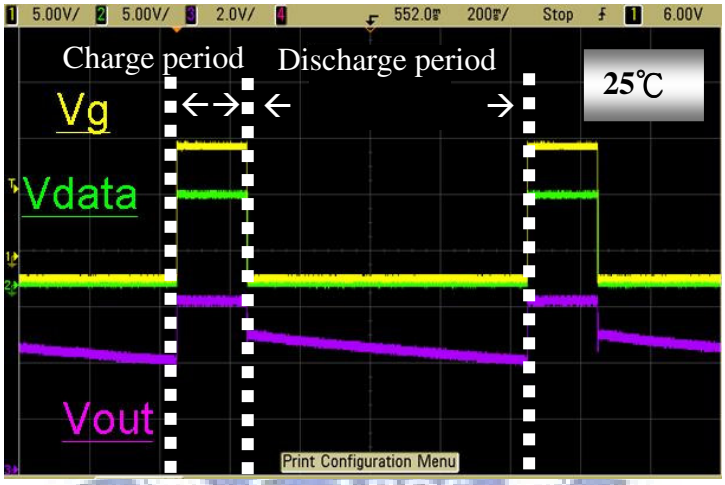

(b)

(c)

Fig. 3-5 (a) Photograph of the fabricated temperature sensor circuit and (b) measured signals of output temperature sensor circuit from oscilloscope at 25℃ and (c) 80℃

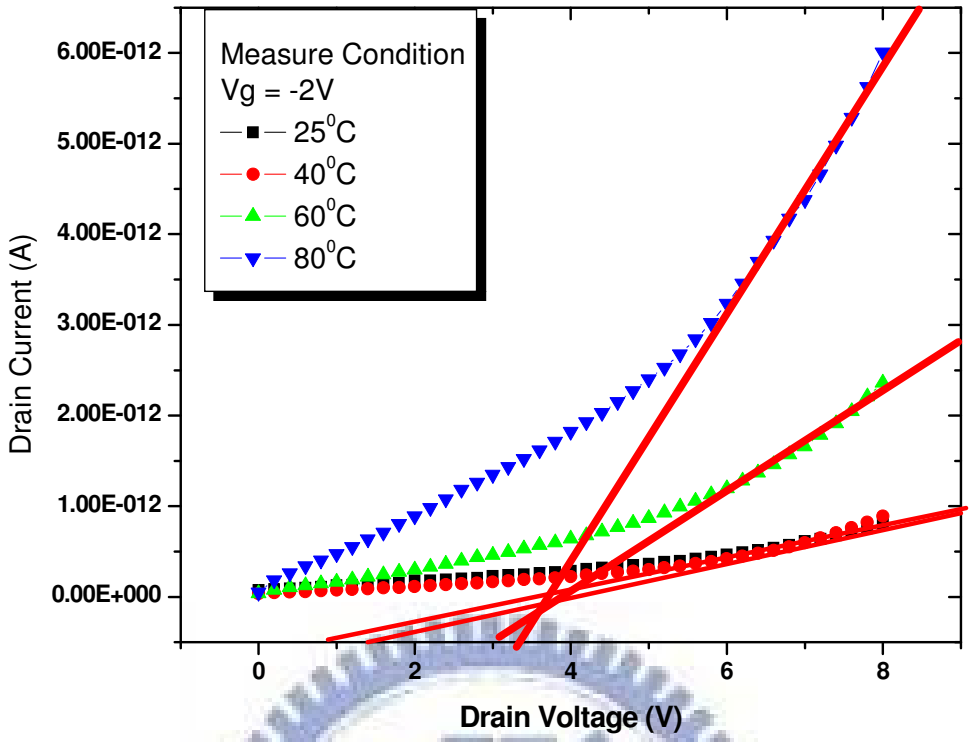

Fig. 3-6 Temperature dependence of I_D - V_D characteristics at V_G = -2V.

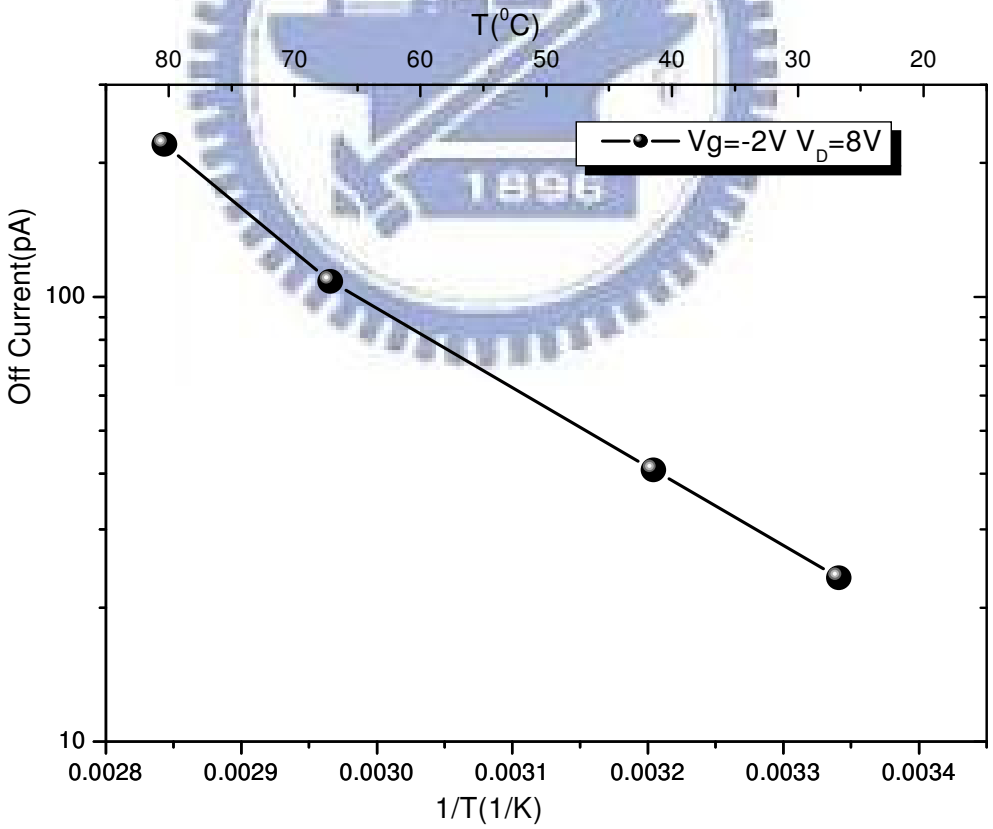

Fig. 3-7 Measured leakage current of temperature sensor circuit at different temperatures.

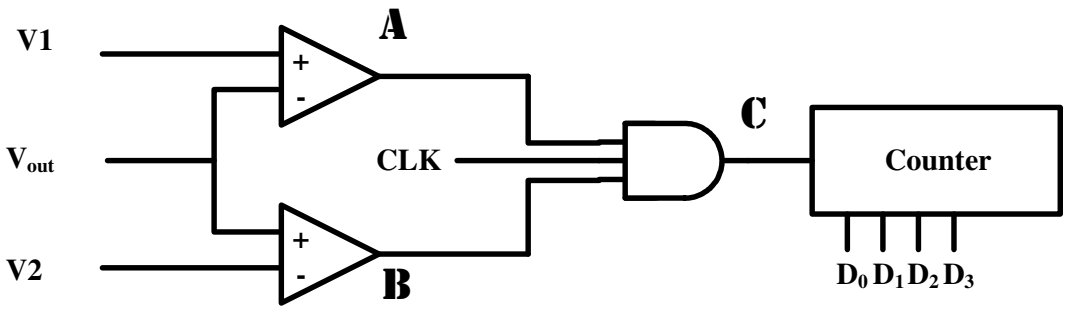

(a)

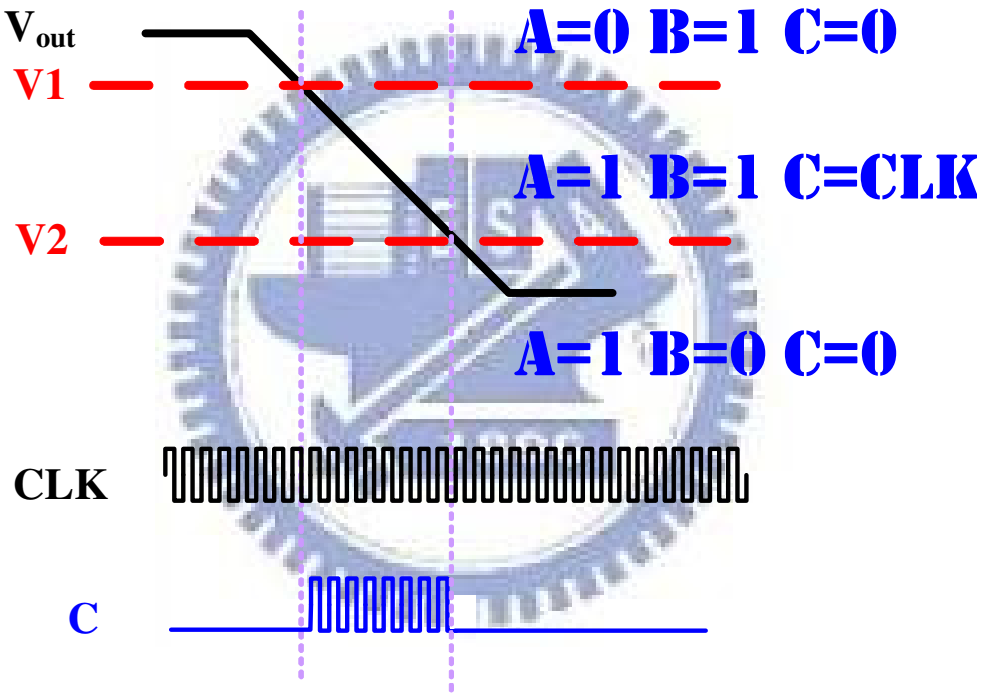

(b)

Fig. 3-8 (a) Simplified block diagram of digitization circuit and (b) its signal diagrams.

Chapter 4

Assessment of the Proposed Circuit

We assess the proposed temperature sensor circuit in the aspect of its accuracy, temperature error. So we will discuss the temperature errors under the two types of device variations, namely, off current variation and Vth variation. In addition we proposed a calibrate method to reduce the sensing error. Then we will discuss the temperature errors again.

4.1 Temperature Error Without Calibration

In the former section, we describe how the temperature sensor circuit works. If we want to commercialize the sensor, we must ensure the accuracy of the sensor. In this section, we discuss the error of temperature sensor arisen by device variation. Two types of the device variation, namely, off current variation and Vth shift, as shown in Fig. 2-7 are considered.

4.1.1 Off Current Variation

Firstly, we measure seven sensors on the same glass at Vg = -2V and V_D = 8V. As shown in Fig. 4-1(a), the measured off currents are very uniform. But when we reduce V_D to 4V, the results become less uniform as shown in Fig. 4-1 (b). Then the sensors on different glasses are measured. As shown in Fig. 4-2, they are much less uniform than those on the same glass. From these three groups of data, we can say that high V_D can reduce off current variation, as long as the variation is not huge among different samples.

4.1.2 Threshold Voltage Variation

Because we don't have two samples with large difference in Vth at hand, we instead change Vg to simulate that if the Vth shifts. Thus we can evaluate the variation under Vth shift.

We measure the temperature sensor circuit at Vg = -1V, -2V, -3V and V_D = 8V. We use it to simulate when the Vth shifts 1V at Vg = -2V. As shown in Fig. 4-3(a), the variation is serious and inevitable. Similarly we measure at V_D = 6V and 4V as shown in Fig. 4-3(b) and Fig. 4-3 (c). Because the current level at low V_D is smaller than at high V_D, when we use lower V_D such as V_D = 4V, the variation is less obvious than high V_D. The impact is more serious than that from off current variation.

4.1.3 Temperature Error Evaluation

To be used as a temperature sensor, we care about mostly its accuracy. Table 4-1 shows temperature errors with respect to the two device variations. According to the data if we consider the off current variation only, the temperature error is 7℃ at V_D = 8V. When V_D decreases to 4V, the error increases to 10℃. If Vth shifts 1V, the temperature error is over 19℃ at V_D = 8V, and the error decreases to 14℃ when V_D=4V.

Therefore, if we want to commercialize the sensor, how to decrease the error is the next problem we must deal with. So we propose a calibrate method to decrease the temperature error.

4.2 Room temperature Calibration

4.2.1 The Principle of Calibration

In Fig. 4-2, we can see that change of currents upon the temperature exhibits

similar trend. All of them are just shift in the current level with each other, while the slope doesn't change among different samples. As we know the temperature dependence of the mobile holes in equilibrium with the trapped charge is given by:

$$I_{off} = I_0 e^{-\frac{Ea}{kT}} \tag{9}$$

I_0 = constant independent of temperature, and

Ea= drain current activation energy which measures the difference between the valence band and the energy of the grain boundary states within kT of the Fermi level [10]. Therefore the slope represents Ea/k and k is Boltzmann constant. Then we can calculate average Ea. The result is shown in Fig. 4-4, Ea is about 0.4eV with error of 0.05eV. So we proposed a calibrate method aim at the current level instead of Ea.

4.2.2 Calibrate Method

Firstly, we assume Ea is constant for all samples and apply the average Ea for calibration. In order to cancel the current level variation among different glasses, we use the ratio of the sensing current to that at room temperature (25℃) as an index expressed as

$$I_{ratio}(T) = \frac{I(T)}{I_{RT}}, \tag{10}$$

where I(T) is the current at different temperature and I_{RT} is the current at room temperature. Fig. 4-5 replots the previous results according to Eq. (10). We call this method "room temperature calibration". The average Ea is used as the basis of sensing, since the reference curve can be expressed as following:

$$I_{refl} = e^{-\frac{\overline{Ea}}{k}(\frac{1}{T}-\frac{1}{RT})} \tag{11}$$

where $\overline{Ea}$ is the average Ea. The reference curve is also plot in Fig. 4-5. In next chapter, we will discuss the error of the proposed circuit based on this reference curve.

4.2.3 Temperature Error after Calibration

4.2.3.1 Off Current Variation

Fig. 4-6 and Fig. 4-7 show the I_{ratio} for V_D=8V, 6V, 4V after normalization. In these figures, the improvement of low V_D is less obvious than high V_D, because the variation is too huge for low V_D. Therefore we won't discuss the temperature error at low V_D later. Next, the reference relation between temperature and off current are created by averaging data from samples on different glasses, as shown in Fig. 4-8.

After that we use the reference curve to be the base of sensing, and than we can get the sensed temperatures. Fig. 4-9 shows the comparison of the real temperatures and the measure temperatures. The calibrate method can reduce the error to 5.932℃ for V_D=8V.

4.2.3.2 Vth Variation

The same calibrate method can be used to calibrate the circuit with Vth variation effect. If Vth shifts, the Ea will not be the same. However the difference of Ea, when Vth shift is 1V, is only 3.47% as shown in Fig. 4-10. So we can imitate the same calibrate method into Vth variation on the proposed sensor circuit.

Fig. 4-11 shows the calibration results for V_D=8V and the reference curves are created as shown in Fig. 4-12. Than by using the reference curve, we get the sensed temperatures. The temperature errors are shown in Fig. 4-13. The error is reduced to 7.849℃ with Vth shift 1V.

4.2.3.3 Average Calibration

For the previous work in our lab (thesis of Yu-Te Chao), we try to use the statistical method to reduce the variation further. We average the measure temperatures in each temperature and use it to be the sensing temperature [11]. After averaging, the temperature errors are shown in Fig. 4-14. Deal with the off current

variation, the error is reduced to 4.405℃. When Vth shift 1V, the error is reduced to 3.853℃.

4.3 Calibration and Error Analysis

If we do not do any calibration for the proposal temperature sensor circuit, the temperature error can be over 7℃. In addition when we consider with the effect of Vth shift, the error will be upon 19℃. However, after room temperature calibration, the errors are decreased to 5.932℃ and 7.849℃ successfully. As long as we average the measure temperatures in each temperature, we can further reduce the error to 4.405℃ and 3.853℃ as shown in Fig. 4-15. Than according to the transmission error, the sum of two errors would be expressed as

$$\sigma_{\text{total}} = \sqrt{\sigma_1^2 + \sigma_2^2}\ . \tag{12}$$

The total temperature error of the proposed sensor circuit is 5.852℃. The proposed circuit with calibration can be a reliable temperature sensor.

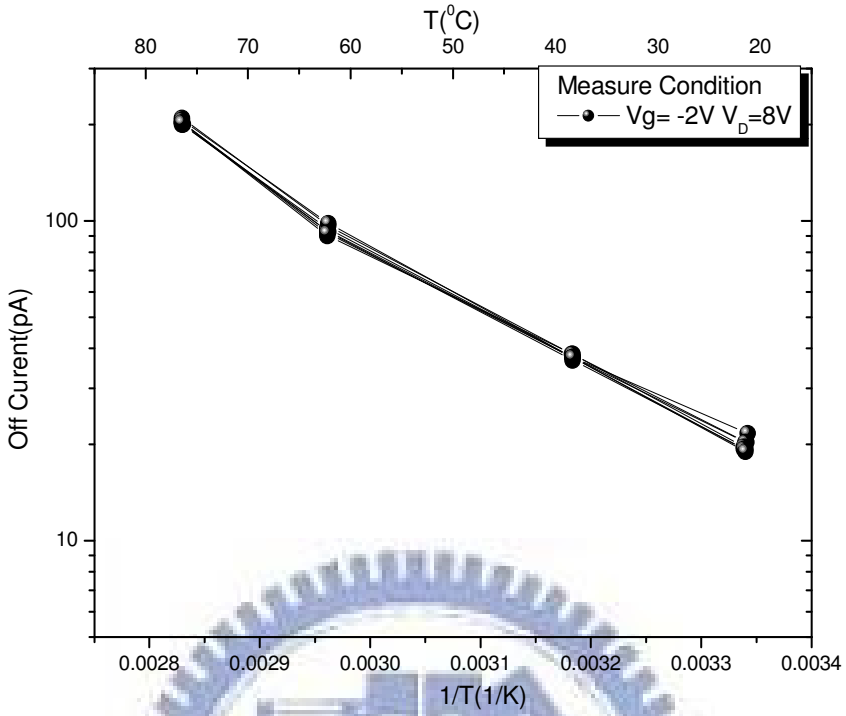

(a)

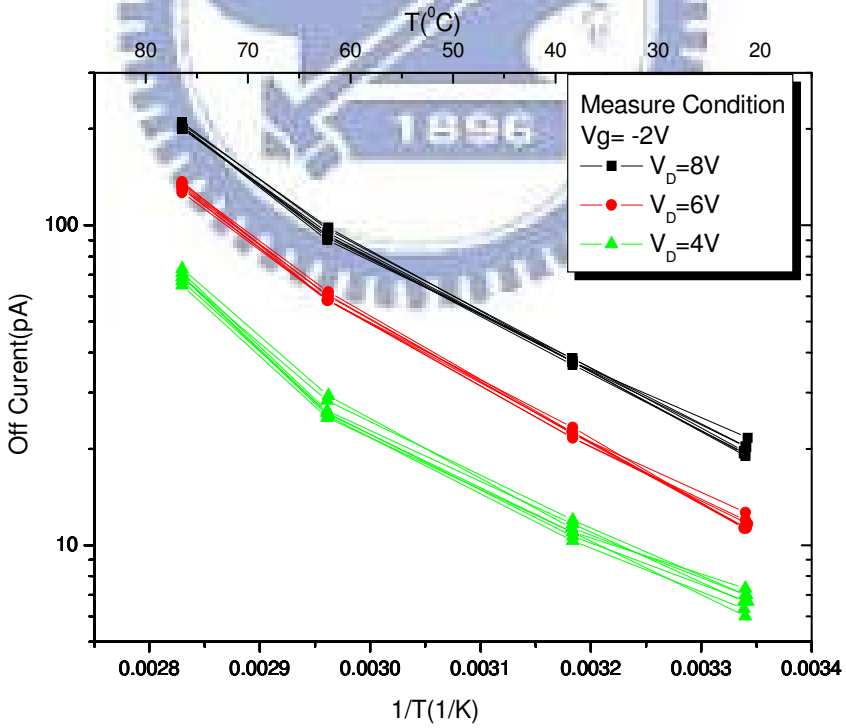

(b)

Fig. 4-1 (a) Measured output current of seven proposed sensors on the same glass with respect to the temperatures. (b) Proposed sensors operate on different V_D.

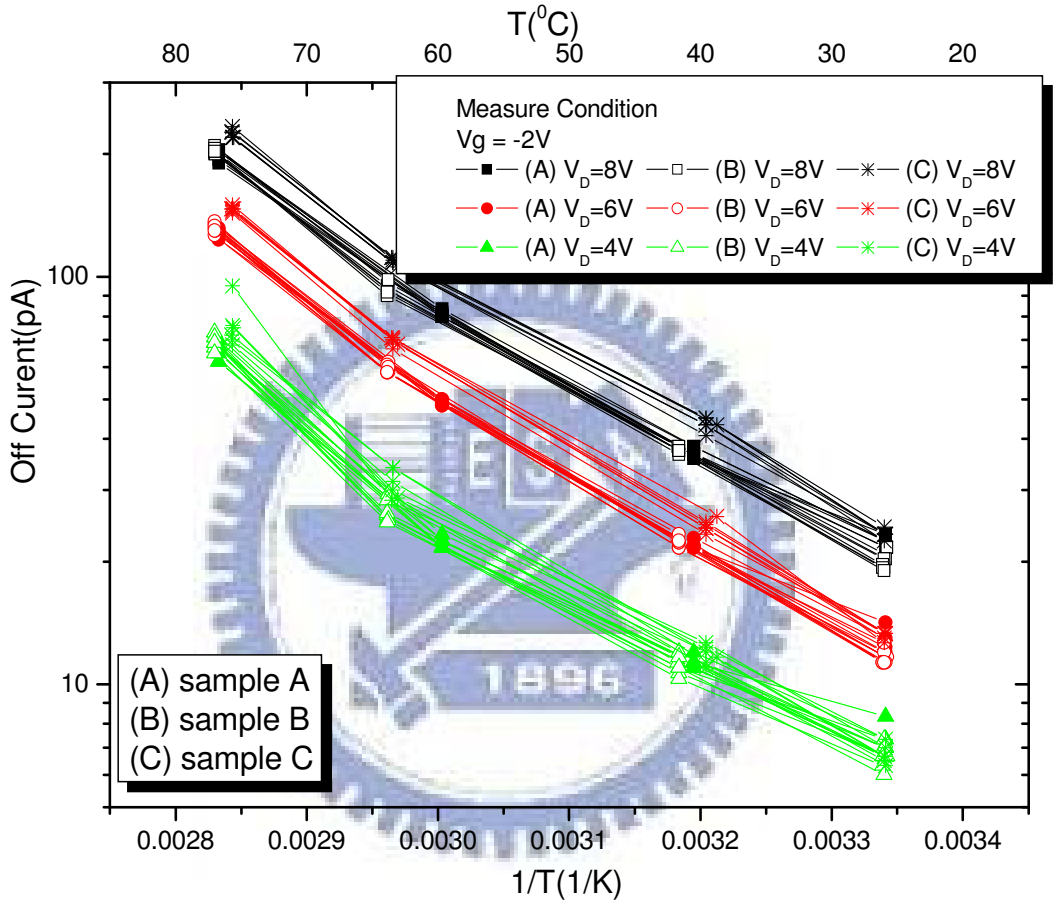

Fig. 4-2 Measured output current of twenty one proposed sensors on three glasses with respect to the temperatures for different V_D.

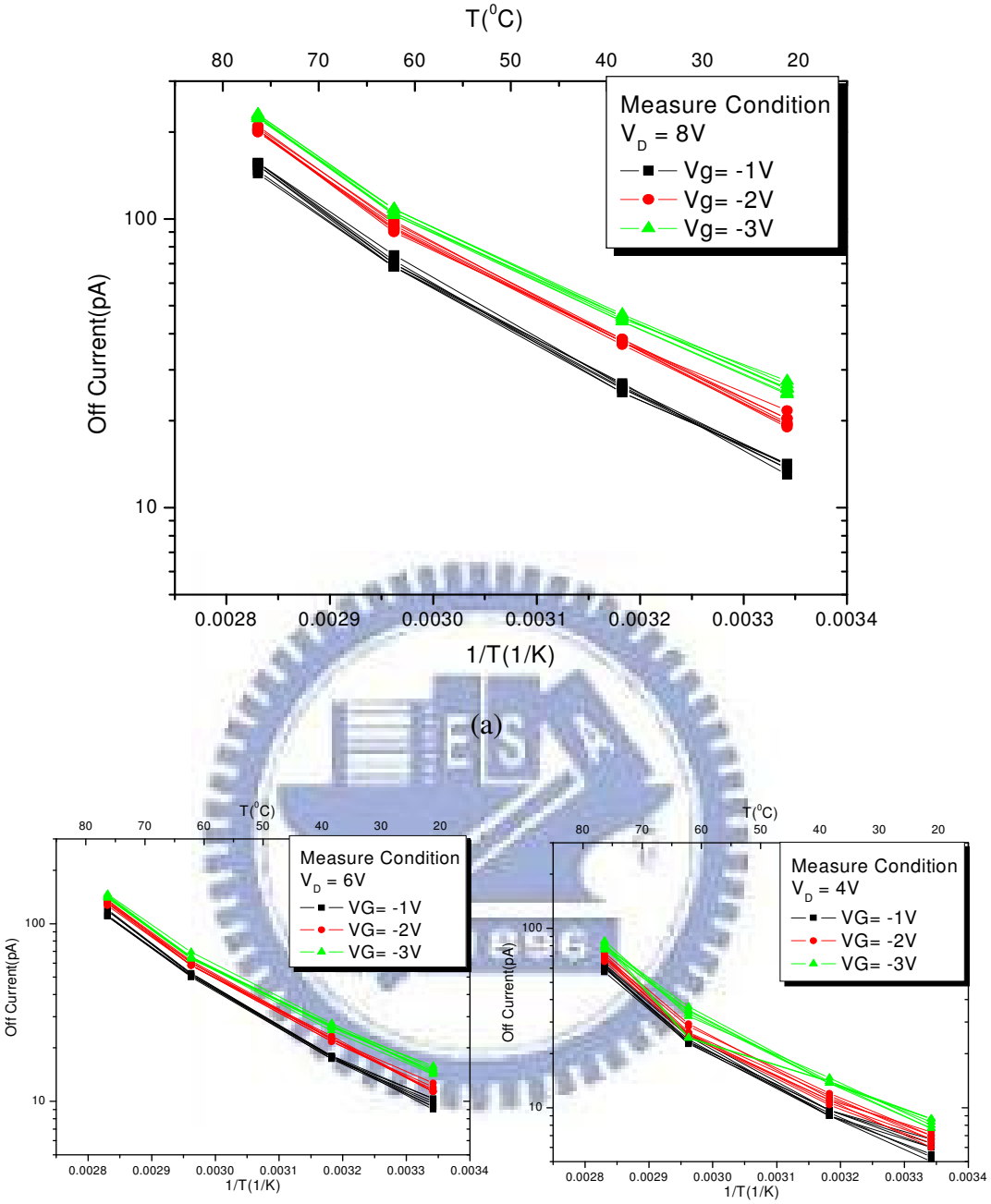

Fig. 4-3 Measured output current of seven proposed sensors on the same glass with respect to the temperatures for different Vg and V_D.

Table 4-1 Temperature errors evaluation.

Experiment	Operator		Temperature Error
Off Current Variation	Vg(V)	V_D(V)	△T(℃)
	-2	8	≒ 7
		6	≒ 8
		4	≒ 10
Vth Shift	△Vg(V)	V_D(V)	△T(℃)
	2(-1 ~ -3)	8	≒ 19
		6	≒ 14
		4	≒ 14

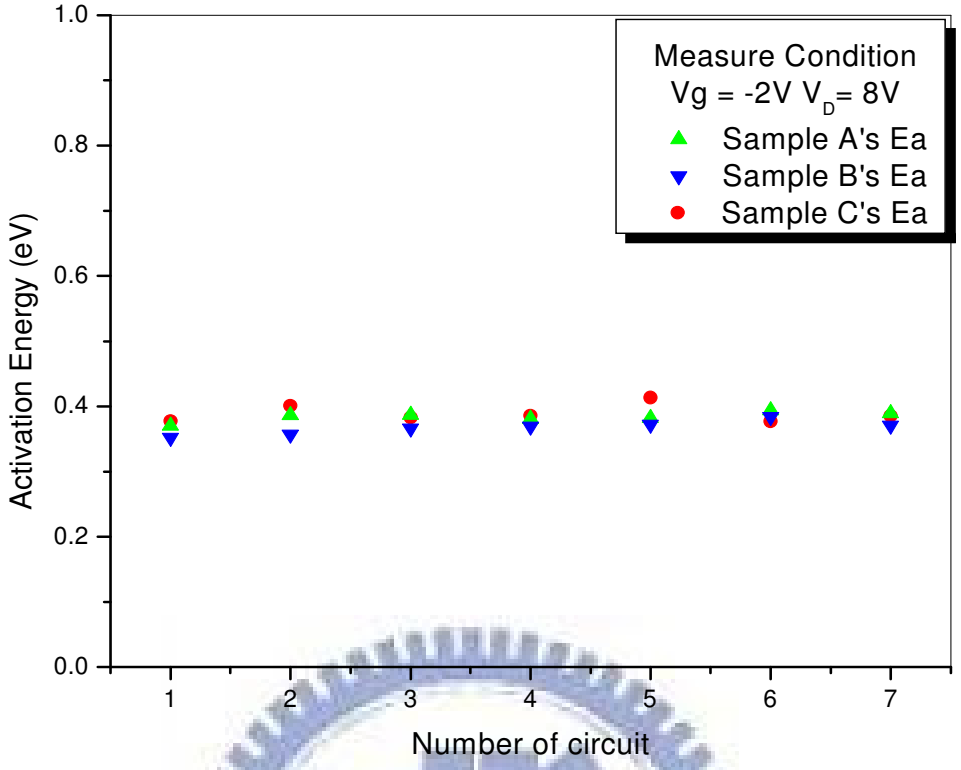

Fig. 4-4 The Ea of device on three glasses.

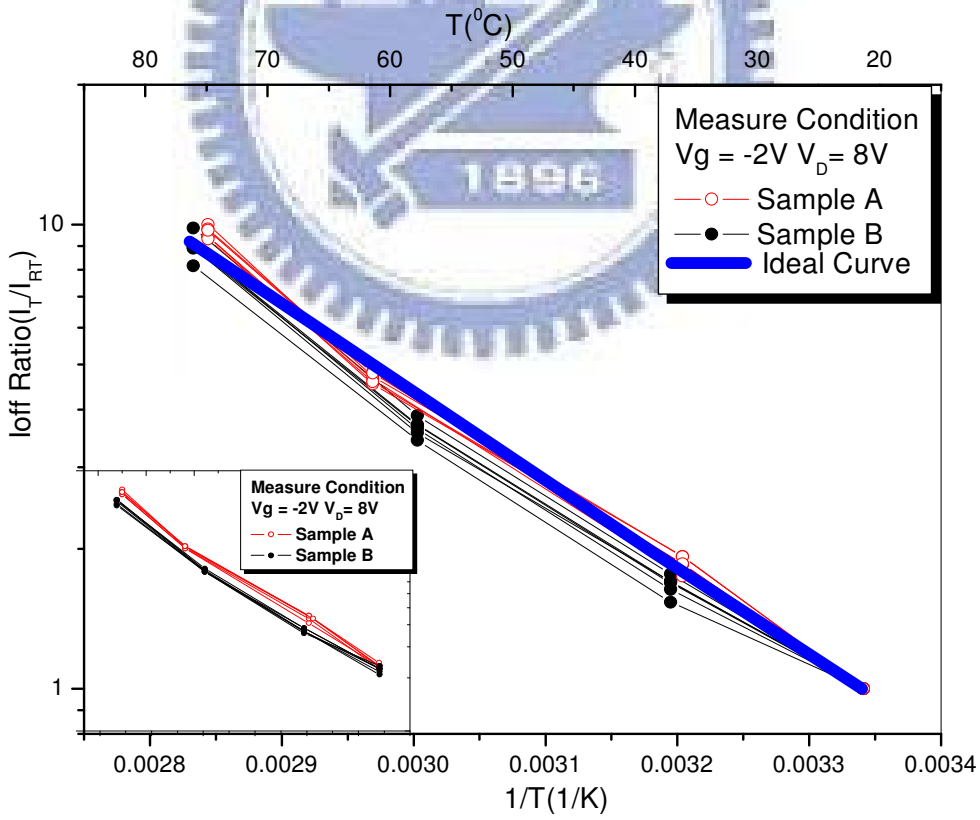

Fig. 4-5 The current ration after room temperature calibration and the inset is the current without calibrate.

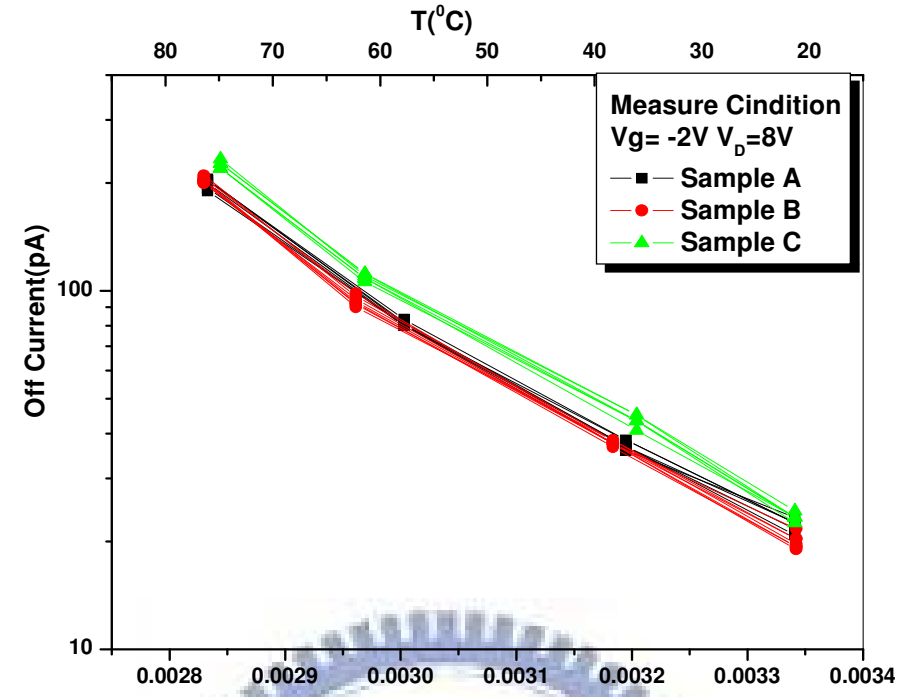

(a)

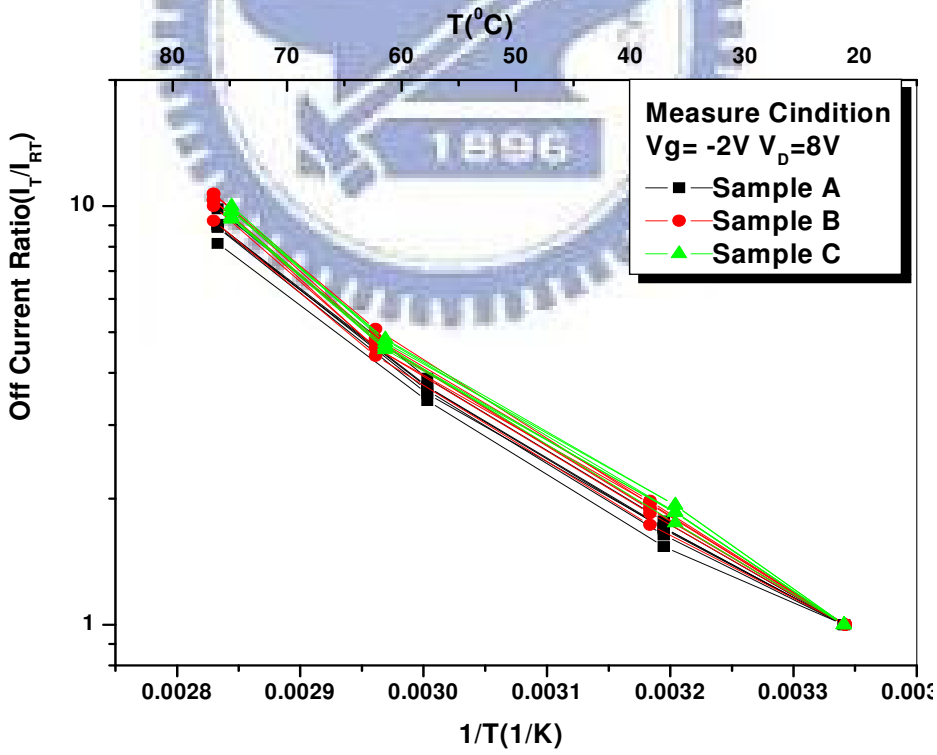

(b)

Fig. 4-6(a) Temperature dependence on the output current on different glasses at Vg = -2V and V_D =8V. (b) The off current ratios after room temperature calibration.

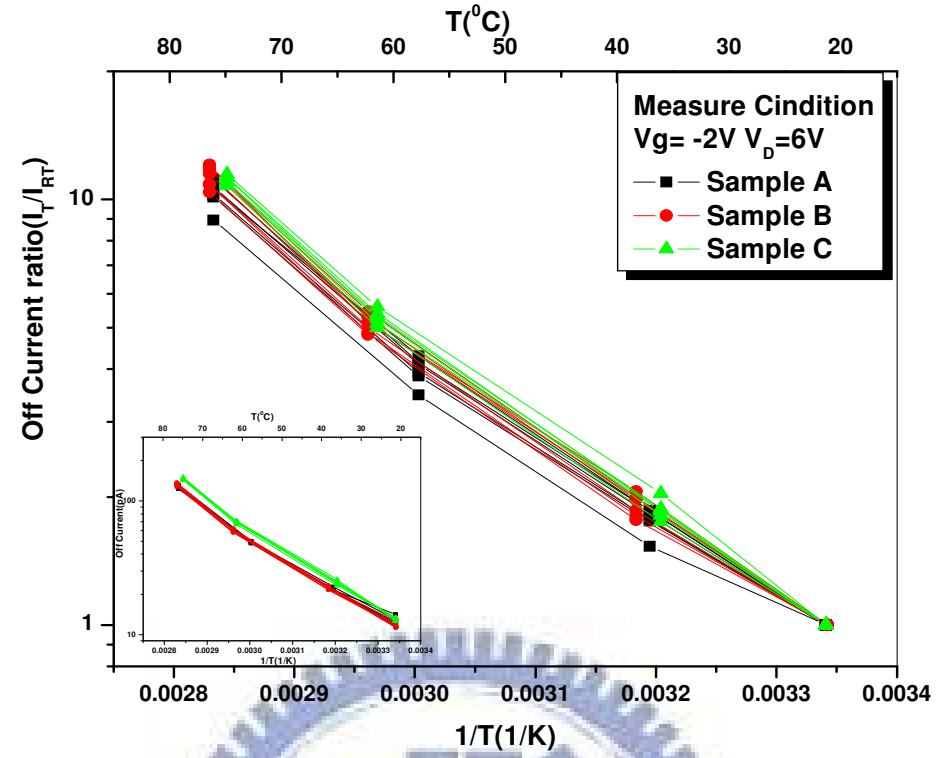

(a)

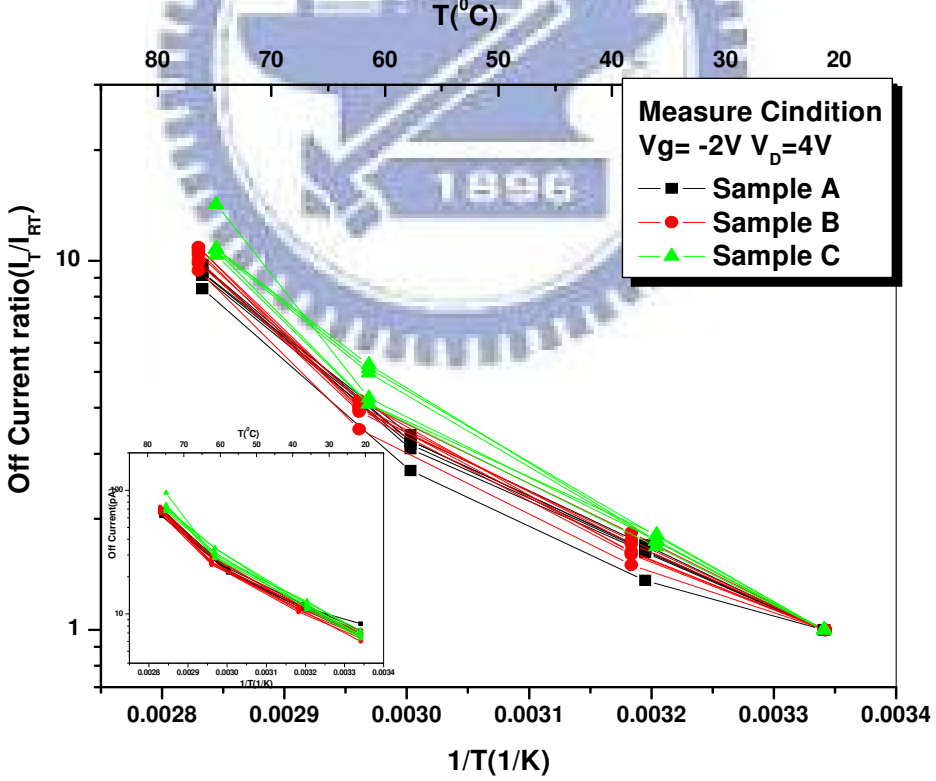

(b)

Fig. 4-7 The off current ratios after room temperature calibration at Vg = -2V and V_D = (a) 6V, (b) 4V. The inset shows the output current without calibration.

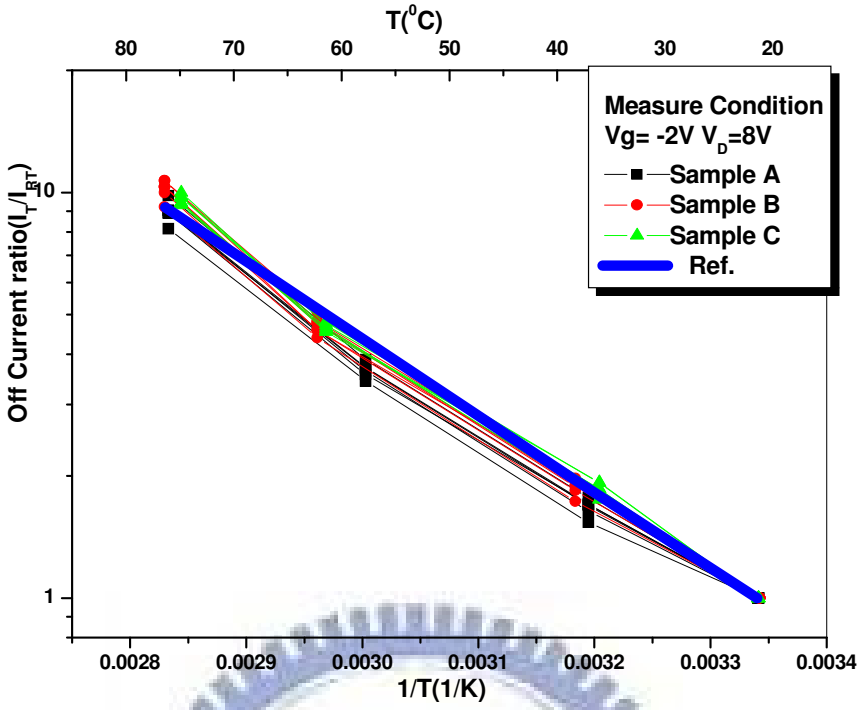

Fig. 4-8 The reference curve of calibration on different glasses at Vg = -2V and V_D = 8V.

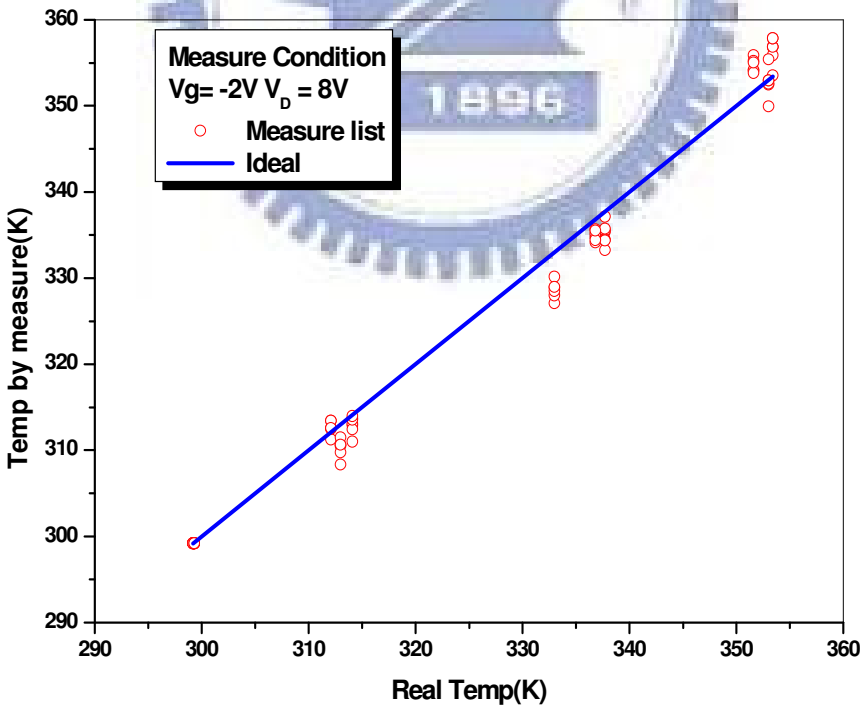

Fig. 4-9 The temperature errors after calibration at Vg= -2V and V_D= 8V.

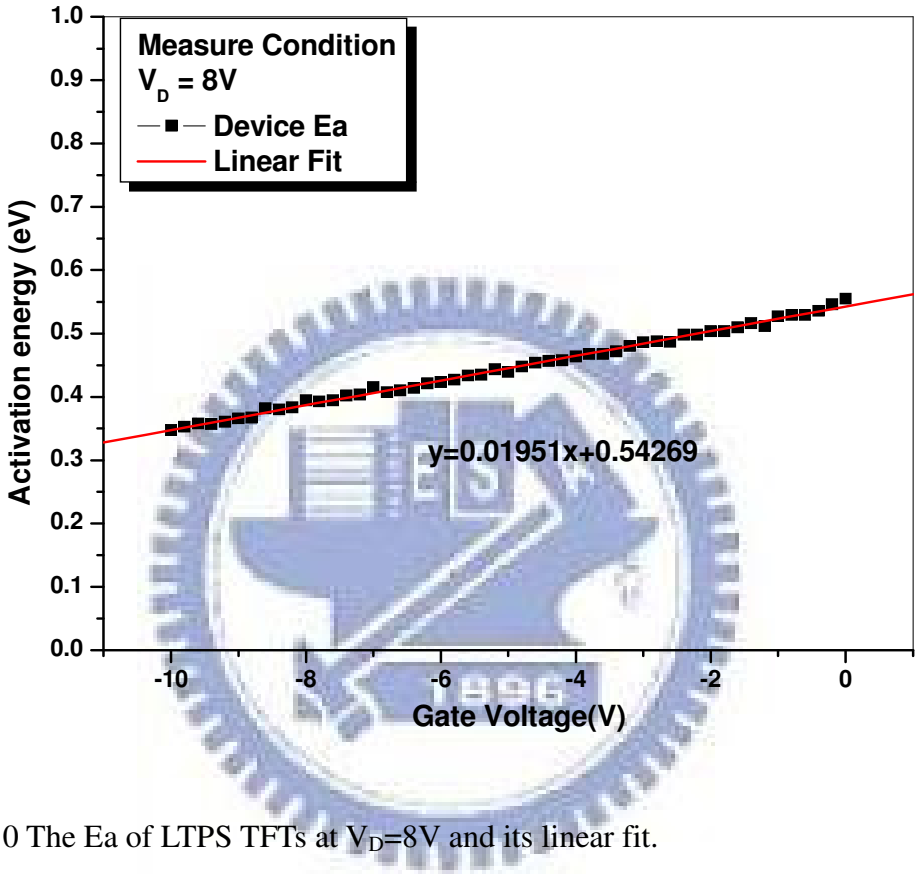

Fig. 4-10 The Ea of LTPS TFTs at V_D=8V and its linear fit.

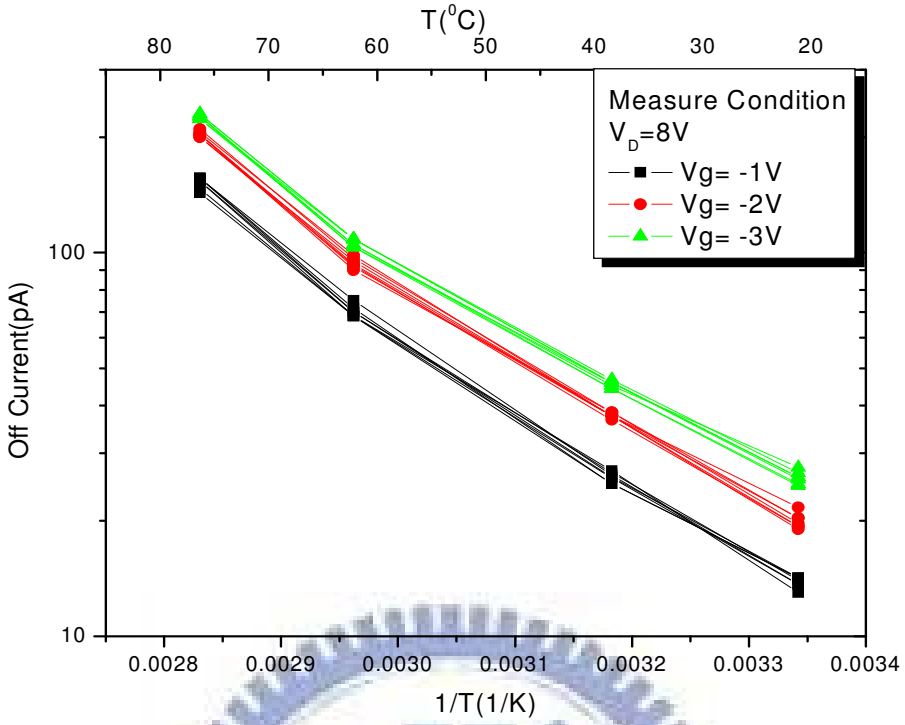

(a)

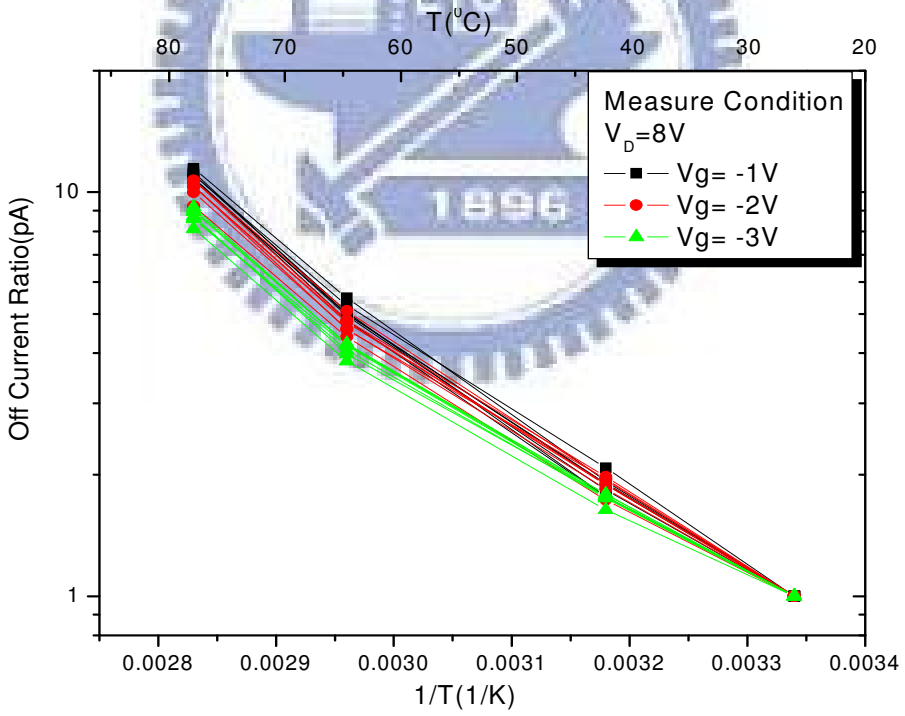

(b)

Fig. 4-11 (a) Temperature dependence on the output current at different Vg and V_D =8V. (b) The off current ratios after room temperature calibration.

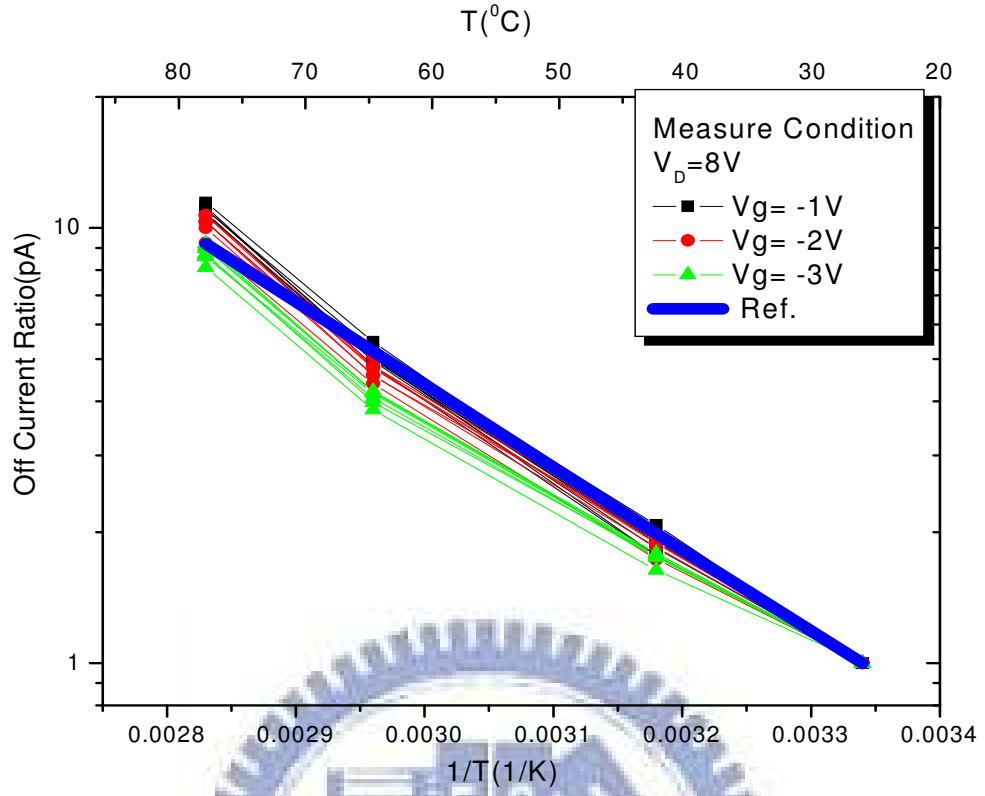

Fig. 4-12 The reference curve of calibration at different Vg and V_D = 8V.

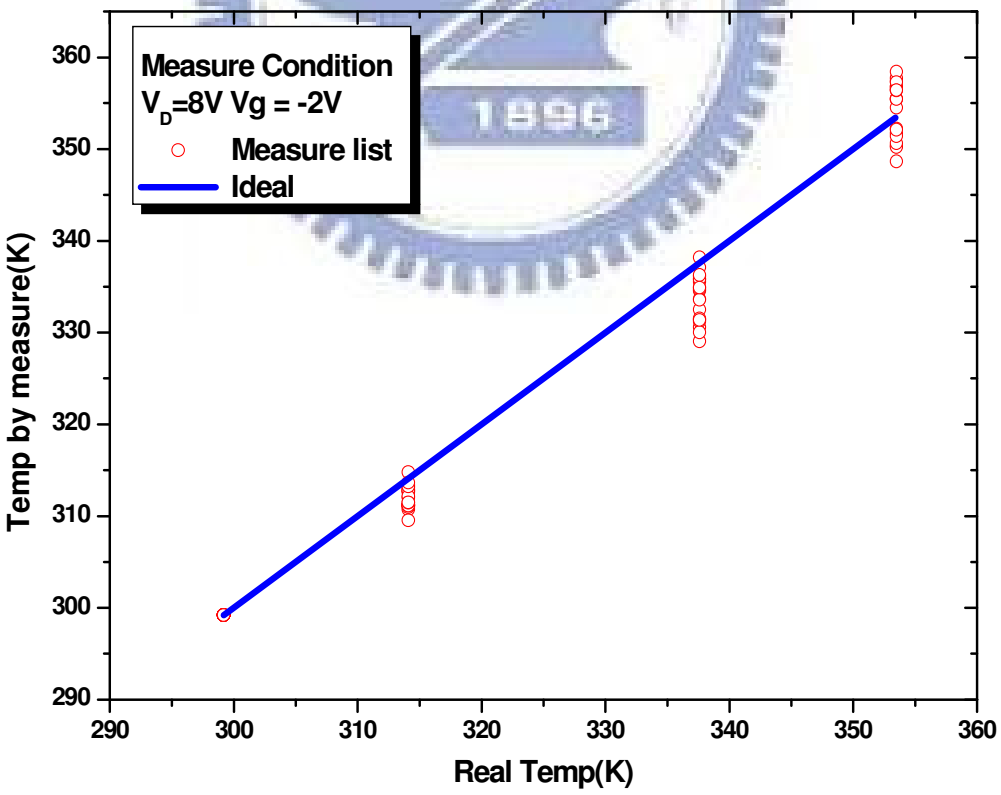

Fig. 4-13 The temperature errors after calibration at Vg= -2V and V_D= 8V.

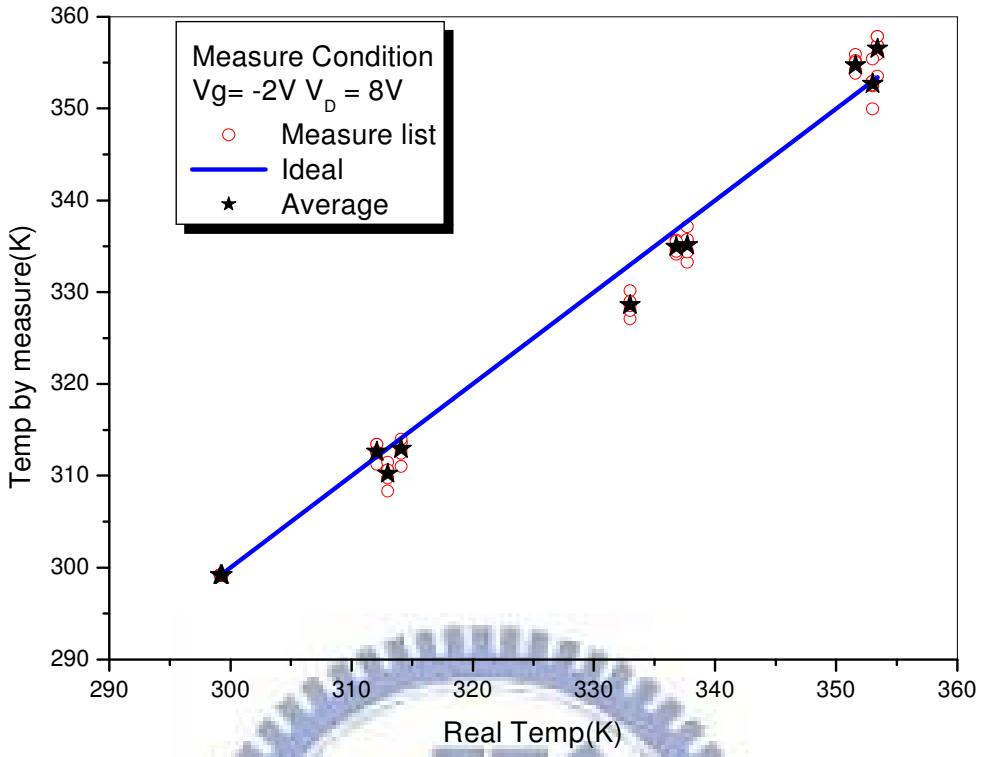

(a)

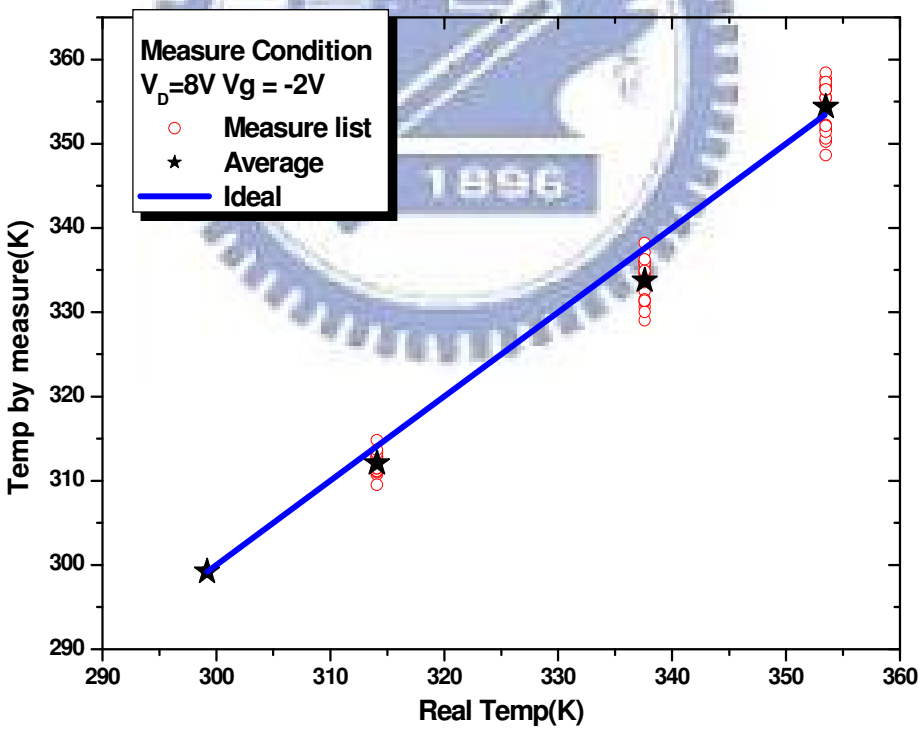

(b)

Fig. 4-14 The temperature errors deal with (a) off current variation and (b) Vth variation after calibration at Vg= -2V and V_D= 8V.

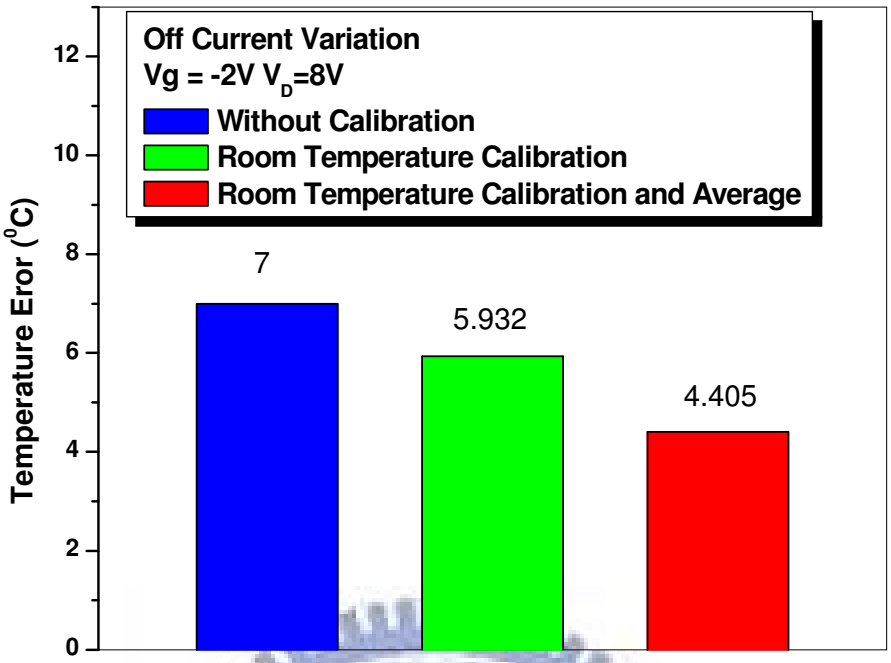

(a)

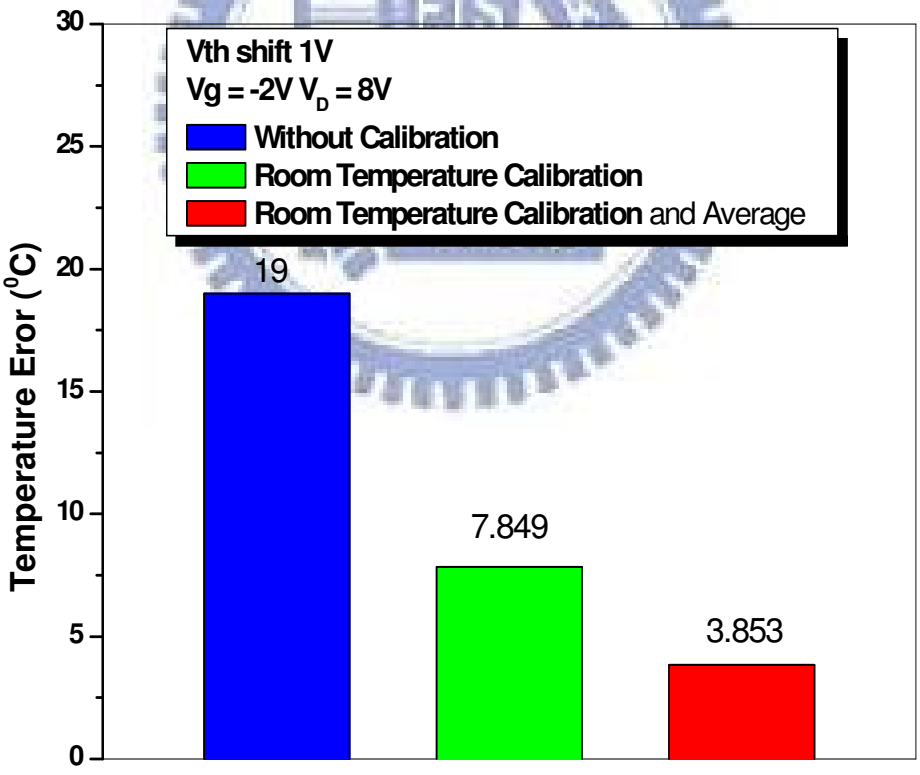

(b)

Fig. 4-15 Temperature errors of proposed sensors deal with (a) off current variation and (b) Vth variation.

Chapter 5

Conclusion

A new temperature sensor is developed by directly using LTPS TFTs identically fabricated with the pixel TFT. Owing to the poor uniformity of LTPS TFTs, a calibrate method considering the off current variation and Vth shift variation, is proposed. It is performed at room temperature. Fig. 5-1 shows the temperature error with calibration cost. Generally we get the reference curve for sensing by sampling. It only need a little cost but the sensing errors is above 20℃. If we calibrate every circuit, the errors would be zero. But it needs a lot of cost. By using room temperature calibration, the error will be reduced to 9.838℃ with some cost. After average calibration, the error can be reduced to 5.852℃ with reasonable cost.

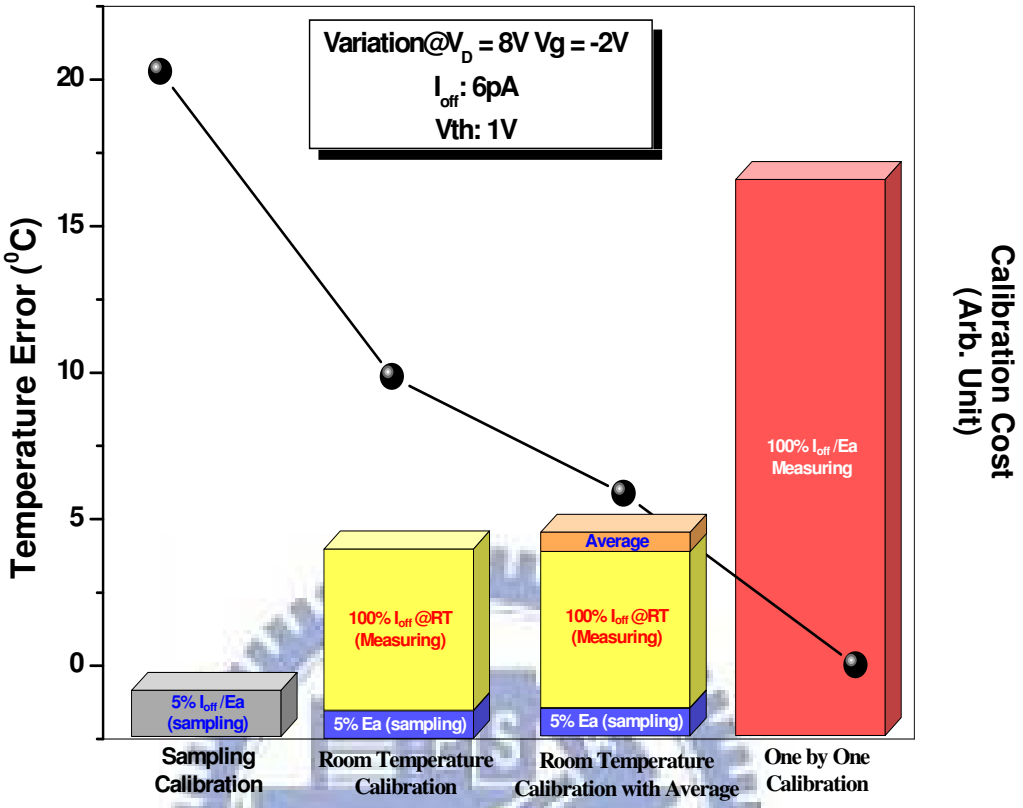

Fig. 5-1 The temperature error with calibration cost.

REFERENCES

[1] S.M. Lee, S.J. Uhm, J.I. Bang, K.D. Song, B.S. Joo, "A field effect transistor type gas sensor based on polyaniline" *IEEE Transactions on Electron Devices,* vol 2, pp. 1935-1938, 2005.

[2] T. Eguchi, Y. Hiyoshi, E. Kanda, H. Sera, T. Ozawa, T. Miyazawa, and T. Matsumoto," A 1300-dpi optical image sensor using an a-Si:H photo diode array driven by LPTS TFTs" *SID Tech. Dig.*, 2007, pp. 1097-1100.

[3] N. Tada, H. Hayashi, M. Yoshida, M Ishikawa, T. Nakamura, T. Motai and T. Nishibe "A Touch Panel Function Integrated LCD Using LTPS Technology," *IDW,* 2004, pp. 349-350.

[4] S. Koide, S.Fujita, T Lto, S. Fujikawa, T. Matsumoto "LTPS Ambient Light Sensor with Temperature Compensation" *IDW, 20*06, pp. 689-690.

[5] S.C. Huang, G.F. Peng, J.L. Chern, Y.H. Tai "Statistical Investigation on the Variation Behavior of Low-Temperature Poly- Si TFTs for Circuit Simulation" *SID Tech. Dig.,* 2006*,* vol 37, pp. 329-332

[6] JW Lee. In: Electron devices meeting, 1998. IEDM 98 Technical Digest, International, 1998

[7] S.M. Sze, Semiconductor Sensor, Wiley-Interscience Publication, New York, 1994.

[8] W.D. Boer, A. Abileah, P. Green, T. Larsson, "Active Matrix LCD with Integrated Optical Touch Screen" *SID Tech. Dig.,* 2003, pp. 1494-1497.

[9] B.T. Chen, Y.H. Tai, K.F. Wei, C.C. Tsai, C.Y. Huang, Y.J. Kuo, H.C. Cheng "Investigation of source-follower type analog buffer using low temperature poly-Si TFTs" *Solid-State Electronics,* vol. 51, pp. 354-359, 2007.

[10] H.-S. Lim and O.K. Kwon “Ambient Light Sensing Circuit with Low-Temperature Polycrystalline Silicon p-Intrinsic-n Diode and Source Follower for Auto Brightness Control” *Japanese Journal Applied Physics,* vol. 47, No 3, pp. 1919-1923, 2008.

[11] K. R. Olasupo and M. K. Hatalis “Leakage Current Mechanism in Sub-Micron Polysilicon Thin-Film Transistors” *IEEE Transactions on Electron Devices*, vol. 43, pp. 1218-1223, 1996.

[12] Y.H. Tai, S.C. Huang, W.P. Chen, Y.T. Chao, Y.P. Chou, and G.F. Peng “A Statistical Model for Simulating the Effect of LTPS TFT Device Variation for SOP Applications” *IEEE Journal of Display Technology*, vol. 3, pp.426-433, 2007.